The current observation raises the possibility that the reduction of HCV load and/or liver inflammation correlates with the increment of Treg frequency, or vice versa. Recently, it was reported that liver inflammation caused by HCV induces PD-L1 on hepatocytes, which then suppress Treg proliferation in liver [26]. If such a scenario is operative as well in PEG-IFNα and ribavirin therapy, alleviation of liver inflammation may reduce PD-L1 expression on hepatocytes, thereby stimulating Treg proliferation. However, most of the TR patients, who were categorized as being in the non-SVR group, displayed normalized serum ALT levels and negative HCV RNA during treatment, of which conditions are equivalent with the SVR patients. Thus, it is still uncertain whether or not such mechanisms are applicable to the present results.

The other possibility is that phenotypically determined Tregs in this study partly consist of activated T cells. It is well known that $CD127^-$ and $FOXP3^+$ are reliable markers of Tregs [27]. In order to examine whether or not the increment of Treg frequency in this study is a contamination of activated T cells, we determined Tregs as $CD4^+CD25^{high}FOXP3^+CD127^-$ cells instead of $CD4^+CD25^{high}$ cells in some patients. In the comparison of the ratio of $CD4^+CD25^{high}FOXP3^+CD127^-$ cell frequency between the SVR and non-SVR groups at T12W, similar results were obtained with those of $CD4^+CD25^{high}$ cells (SVR vs. non-SVR, 10 patients in each group, 2.50 ± 1.20 vs. 1.54 ± 0.53, $P < 0.05$ by Mann–Whitney U test). These results suggest that the analytical results of $CD4^+CD25^{high}$ T cells reflect those of $FOXP3^+$ Tregs. Further investigation is needed to show that such Tregs are functionally suppressive and to see if the change of frequency parallels with suppressor capacity or not.

According to the AASLD practice guidelines for the treatment of chronic hepatitis C, a combination of PEG/R for 48 weeks is recommended for patients who attained c-EVR at week 12 of therapy [17]. However, in some cohorts with large numbers of patients, approximately 30% of them eventually relapse after cessation of the therapy [5]. The factors involved in post-therapeutic relapse have not been fully explored. We and others have reported that liver fibrosis, female gender, late virological response, and dosage of ribavirin (drug adherence) are critically involved in relapse [19, 28, 29]. It is well known that platelet counts in patients with chronic liver disease are well correlated with the degree of fibrosis. In the present study, multivariate analyses revealed that platelet counts but not fibrosis stage are involved in SVR. The reasons for such discrepant contributions to SVR are not clear; however, it demonstrates that the degree of fibrosis is involved in the therapeutic response in this cohort. In addition, the current study showed that the changes of PDC frequency are also somewhat involved in virological relapse in patients that once attained c-EVR.

Plasmacytoid DCs (PDC) play crucial roles in antivirus immune responses by producing IFN-β and -α [30]. In the previous study by us [14], the increment of PDC is observed in patients with SVR, of which change is more significant in those with c-EVR. No concrete explanation is available for the mechanisms of PDC increase in SVR patients. One of the possibilities is that the PDC increase is a consequence of better response to exogenous IFN-α in patients who have a higher chance of attaining SVR. IFN-α is reported to act as a regulatory factor on $CD11c^-$ DCs to sustain their viability and to inhibit gaining the ability to stimulate Th2 development [31]. Such a possibility is supported by the findings that higher induction of IFN-stimulated genes (ISGs) in hepatocytes after PEG-IFNα and ribavirin therapy, but not higher ISG levels before therapy, is critically involved in successful outcome [32]. Thus, patients who respond well to IFN-α, as demonstrated by better PDC survival during the treatment, are likely to have better chances to eradicate HCV.

Another possible reason for the PDC increase in the periphery of SVR patients is that PDC alter their localization during the treatment. Mengshol et al. [33] reported that PDC and myeloid DC (MDC) are accumulated in inflamed liver through the interactions of chemokines and their receptors. Of particular interest is that the expression of such chemokine receptors on DCs decreased in SVR patients, but not in non-SVR ones [33]. Therefore, it is plausible that PDC may migrate from the liver to periphery/lymphoid tissue after being unleashed from chemokines in the liver. In support for this, it is reported that IFN-α alters the profiles of chemokine receptors on DC, resulting in changes of the DC migrating ability [34].

Recently, numerous other factors were reported to be involved in therapeutic response in chronic hepatitis C patients, such as mutations of HCV genome (core region) [35] or host genetic variation (single nucleotide polymorphisms near the IL28B gene) [36]. In the current study, we were unable to analyze such factors because of the limited numbers of patients. A prospective study is warranted to analyze the involvement of such factors in relation to immune cell markers, in the outcomes of SOC, or the treatment with direct-acting antiviral agents.

In summary, we demonstrated that the increase of Treg frequency is an independent factor involved in SVR in 48 weeks of SOC for chronic hepatitis C patients. In addition, the increase of PDC gains similar significance in SVR patients who attained c-EVR. The assessment of the dynamics of such cells during therapy could offer some clues to identify potential relapsers and give them a better chance of attaining SVR by rescheduling the therapy.

Acknowledgments This study was funded in part by Grant-in-Aid Ministry of Health, Labor and Welfare of Japan and Ministry of Education, Science and Culture of Japan (ID: 22590729 and 22590730).

Conflict of interest The authors declare that they have no conflict of interest.

References

1. Nordenstedt H, White DL, El-Serag HB. The changing pattern of epidemiology in hepatocellular carcinoma. Dig Liver Dis. 2010;42(Suppl 3):S206–14.
2. Kanwal F, Hoang T, Kramer JR, Asch SM, Goetz MB, Zeringue A, et al. Increasing prevalence of HCC and cirrhosis in patients with chronic hepatitis C virus infection. Gastroenterology. 2010:140: 1182–8.e1.
3. Poynard T, Colombo M, Bruix J, Schiff E, Terg R, Flamm S, et al. Peginterferon alfa-2b and ribavirin: effective in patients with hepatitis C who failed interferon alfa/ribavirin therapy. Gastroenterology. 2009;136:1618–28.e2.
4. Jacobson IM. Treatment options for patients with chronic hepatitis C not responding to initial antiviral therapy. Clin Gastroenterol Hepatol. 2009;7:921–30.
5. Hayashi N, Takehara T. Antiviral therapy for chronic hepatitis C: past, present, and future. J Gastroenterol. 2006;41:17–27.
6. Poynard T. Treatment of hepatitis C virus: the first decade. Semin Liver Dis. 2004;24(Suppl 2):19–24.
7. Davis GL, Wong JB, McHutchison JG, Manns MP, Harvey J, Albrecht J. Early virologic response to treatment with peginterferon alfa-2b plus ribavirin in patients with chronic hepatitis C. Hepatology. 2003;38:645–52.
8. Ferenci P, Fried MW, Shiffman ML, Smith CI, Marinos G, Goncales FL Jr, et al. Predicting sustained virological responses in chronic hepatitis C patients treated with peginterferon alfa-2a (40 KD)/ribavirin. J Hepatol. 2005;43:425–33.
9. Berg T, von Wagner M, Nasser S, Sarrazin C, Heintges T, Gerlach T, et al. Extended treatment duration for hepatitis C virus type 1: comparing 48 versus 72 weeks of peginterferon-alfa-2a plus ribavirin. Gastroenterology. 2006;130:1086–97.
10. Rehermann B. Hepatitis C virus versus innate and adaptive immune responses: a tale of coevolution and coexistence. J Clin Invest. 2009;119:1745–54.
11. Kanto T, Hayashi N. Immunopathogenesis of hepatitis C virus infection: multifaceted strategies subverting innate and adaptive immunity. Intern Med. 2006;45:183–91.
12. Kamal SM, Fehr J, Roesler B, Peters T, Rasenack JW. Peginterferon alone or with ribavirin enhances HCV-specific CD4 T-helper 1 responses in patients with chronic hepatitis C. Gastroenterology. 2002;123:1070–83.
13. Pachiadakis I, Chokshi S, Cooksley H, Farmakiotis D, Sarrazin C, Zeuzem S, et al. Early viraemia clearance during antiviral therapy of chronic hepatitis C improves dendritic cell functions. Clin Immunol. 2009;131:415–25.
14. Itose I, Kanto T, Inoue M, Miyazaki M, Miyatake H, Sakakibara M, et al. Involvement of dendritic cell frequency and function in virological relapse in pegylated interferon-alpha and ribavirin therapy for chronic hepatitis C patients. J Med Virol. 2007;79:511–21.
15. Pawlotsky JM, Bouvier-Alias M, Hezode C, Darthuy F, Remire J, Dhumeaux D. Standardization of hepatitis C virus RNA quantification. Hepatology. 2000;32:654–9.
16. Desmet VJ, Gerber M, Hoofnagle JH, Manns M, Scheuer PJ. Classification of chronic hepatitis: diagnosis, grading and staging. Hepatology. 1994;19:1513–20.
17. Ghany MG, Strader DB, Thomas DL, Seeff LB. Diagnosis, management, and treatment of hepatitis C: an update. Hepatology. 2009;49:1335–74.
18. Oze T, Hiramatsu N, Yakushijin T, Kurokawa M, Igura T, Mochizuki K, et al. Pegylated interferon alpha-2b (Peg-IFN alpha-2b) affects early virologic response dose-dependently in patients with chronic hepatitis C genotype 1 during treatment with Peg-IFN alpha-2b plus ribavirin. J Viral Hepat. 2009;16:578–85.
19. Hiramatsu N, Oze T, Yakushijin T, Inoue Y, Igura T, Mochizuki K, et al. Ribavirin dose reduction raises relapse rate dose-dependently in genotype 1 patients with hepatitis C responding to pegylated interferon alpha-2b plus ribavirin. J Viral Hepat. 2009;16:586–94.
20. Itose I, Kanto T, Kakita N, Takebe S, Inoue M, Higashitani K, et al. Enhanced ability of regulatory T cells in chronic hepatitis C patients with persistently normal alanine aminotransferase levels than those with active hepatitis. J Viral Hepat. 2009;16:844–52.
21. Kanto T, Hayashi N, Takehara T, Tatsumi T, Kuzushita N, Ito A, et al. Impaired allostimulatory capacity of peripheral blood dendritic cells recovered from hepatitis C virus-infected individuals. J Immunol. 1999;162:5584–91.
22. Sugimoto K, Ikeda F, Stadanlick J, Nunes FA, Alter HJ, Chang KM. Suppression of HCV-specific T cells without differential hierarchy demonstrated ex vivo in persistent HCV infection. Hepatology. 2003;38:1437–48.
23. Soldevila B, Alonso N, Martinez-Arconada MJ, Morillas RM, Planas R, Sanmarti AM, et al. A prospective study of T- and B-lymphocyte subpopulations, CD81 expression levels on B cells and regulatory CD4(+) CD25(+) CD127(low/−) FoxP3(+) T cells in patients with chronic HCV infection during pegylated interferon-alpha2a plus ribavirin treatment. J Viral Hepat. 2011;18:384–92.
24. Akiyama M, Ichikawa T, Miyaaki H, Motoyoshi Y, Takeshita S, Ozawa E, et al. Relationship between regulatory T cells and the combination of pegylated interferon and ribavirin for the treatment of chronic hepatitis type C. Intervirology. 2010;53:154–60.
25. Burton JR Jr, Klarquist J, Im K, Smyk-Pearson S, Golden-Mason L, Castelblanco N, et al. Prospective analysis of effector and regulatory CD4+ T cells in chronic HCV patients undergoing combination antiviral therapy. J Hepatol. 2008;49:329–38.
26. Franceschini D, Paroli M, Francavilla V, Videtta M, Morrone S, Labbadia G, et al. PD-L1 negatively regulates CD4+CD25+ Foxp3+Tregs by limiting STAT-5 phosphorylation in patients chronically infected with HCV. J Clin Invest. 2009;119:551–64.
27. Liu W, Putnam AL, Xu-Yu Z, Szot GL, Lee MR, Zhu S, et al. CD127 expression inversely correlates with FoxP3 and suppressive function of human CD4+ T reg cells. J Exp Med. 2006;203: 1701–11.
28. Oze T, Hiramatsu N, Yakushijin T, Mochizuki K, Oshita M, Hagiwara H, et al. Indications and limitations for aged patients with chronic hepatitis C in pegylated interferon alfa-2b plus ribavirin combination therapy. J Hepatol. 2011;54:604–11.
29. McHutchison JG, Manns M, Patel K, Poynard T, Lindsay KL, Trepo C, et al. Adherence to combination therapy enhances sustained response in genotype-1-infected patients with chronic hepatitis C. Gastroenterology. 2002;123:1061–9.
30. Gilliet M, Cao W, Liu YJ. Plasmacytoid dendritic cells: sensing nucleic acids in viral infection and autoimmune diseases. Nat Rev Immunol. 2008;8:594–606.
31. Ito T, Amakawa R, Inaba M, Ikehara S, Inaba K, Fukuhara S. Differential regulation of human blood dendritic cell subsets by IFNs. J Immunol. 2001;166:2961–9.
32. Sarasin-Filipowicz M, Oakeley EJ, Duong FH, Christen V, Terracciano L, Filipowicz W, et al. Interferon signaling and treatment outcome in chronic hepatitis C. Proc Natl Acad Sci U S A. 2008;105:7034–9.

33. Mengshol JA, Golden-Mason L, Castelblanco N, Im KA, Dillon SM, Wilson CC, et al. Impaired plasmacytoid dendritic cell maturation and differential chemotaxis in chronic hepatitis C virus: associations with antiviral treatment outcomes. Gut. 2009;58:964–73.
34. Cicinnati VR, Kang J, Sotiropoulos GC, Hilgard P, Frilling A, Broelsch CE, et al. Altered chemotactic response of myeloid and plasmacytoid dendritic cells from patients with chronic hepatitis C: role of alpha interferon. J Gen Virol. 2008;89:1243–53.
35. Akuta N, Suzuki F, Kawamura Y, Yatsuji H, Sezaki H, Suzuki Y, et al. Predictive factors of early and sustained responses to peginterferon plus ribavirin combination therapy in Japanese patients infected with hepatitis C virus genotype 1b: amino acid substitutions in the core region and low-density lipoprotein cholesterol levels. J Hepatol. 2007;46:403–10.
36. Tanaka Y, Nishida N, Sugiyama M, Kurosaki M, Matsuura K, Sakamoto N, et al. Genome-wide association of IL28B with response to pegylated interferon-alpha and ribavirin therapy for chronic hepatitis C. Nat Genet. 2009;41:1105–9.

IJC
International Journal of Cancer

Comparative analyses of regulatory T cell subsets in patients with hepatocellular carcinoma: A crucial role of $CD25^{-}FOXP3^{-}$ T cells

Naruyasu Kakita[1], Tatsuya Kanto[1,2], Ichiyo Itose[3], Shoko Kuroda[1], Michiyo Inoue[1], Tokuhiro Matsubara[1], Koyo Higashitani[1], Masanori Miyazaki[1], Mitsuru Sakakibara[1], Naoki Hiramatsu[1], Tetsuo Takehara[1], Akinori Kasahara[4] and Norio Hayashi[3]

[1] Department of Gastroenterology and Hepatology, Osaka University Graduate School of Medicine, Suita, Japan
[2] Department of Dendritic cell Biology and Clinical Applications, Osaka University Graduate School of Medicine, Suita, Japan
[3] Kansai Rosai Hospital, Amagasaki, Japan
[4] Department of General Medicine, Osaka University Hospital, Suita, Japan

Regulatory T cells (Tregs) play pivotal role in cancer-induced immunoediting. Increment of $CD25^{high+}FOXP3^{+}$ natural Tregs has been reported in patients with hepatocellular carcinoma (HCC); however, the involvement of other type of Tregs remain elusive. We aimed to clarify whether $FOXP3^{-}$ Tregs are increased and functionally suppressive or not in patients with HCC. We enrolled 184 hepatitis C-infected patients with chronic liver diseases or HCC, 57 healthy subjects and 27 HCC patients with other etiology. Distinct Treg subsets were phenotypically identified by the expression of CD4, CD25, CD127 and forkhead/winged helix transcription factor (FOXP3). Their gene profiles, frequency and suppressor functions against T cell proliferation were compared among the subjects. To examine the molecules involving in Treg differentiation, we cultured naive $CD4^{+}$ T cells in the presence of HCC cells and dendritic cells. We determined two types of $CD4^{+}CD127^{-}$ T cells with comparable regulatory ability; one is $CD25^{high+}$ cells expressing FOXP3 ($CD25^{high+}FOXP3^{+}$ Tregs) and the other is $CD25^{-}$ cells without $FOXP3^{-}$ expression ($CD25^{-}FOXP3^{-}$ cells). The peripheral or intrahepatic frequency of $CD25^{-}FOXP3^{-}$ Tregs in HCC patients is higher than those in other groups, of which significance is more than $CD25^{high+}FOXP3^{+}$ cells. Of importance, $CD25^{-}FOXP3^{-}$ Tregs, but not $CD25^{high+}FOXP3^{+}$ cells, dynamically change in patients accompanied by the ablation or the recurrence of HCC. $CD25^{-}FOXP3^{-}$ T cells with $CD127^{-}IL\text{-}10^{+}$ phenotype are inducible *in vitro* from naive $CD4^{+}$ T cells, in which programmed cell death 1 ligand 1, immunoglobulin-like transcript 4 and human leukocyte antigen G are involved.. In conclusion, $CD25^{-}FOXP3^{-}$ Tregs with suppressive capacity are increased in patients with HCC, suggesting their distinct roles from $CD25^{+}FOXP3^{+}$ Tregs.

Hepatocellular carcinoma (HCC) is the fifth most common cancer and the third leading cause of cancer-related deaths in the world.[1] One of the most prevalent risk factors for HCC is hepatotropic viruses, such as hepatitis B (HBV) or C (HCV) virus.[2,3] In the process of HCC development, the involvement of tumor-induced immune suppression; *i.e.*, immunoediting, has been implicated. Regulatory T cells (Tregs) are unique subset of T cells, playing essential roles in the maintenance of immune homeostasis or in the protection of hosts from virulent infections and cancers.[4] Generally, the existence of two types of Tregs has been reported. One is naturally occurring $CD4^{+}CD25^{high+}$ Tregs, which are derived from the thymus and suppress auto-reactive T cells. The other is inducible or adaptive Tregs, including interleukin (IL)-10-secreting type-1 regulatory T cells (Tr1) and transforming growth factor (TGF)-β-producing Th3. These are inducible in the

Key words: HCC, regulatory T cells, FOXP3, CD25, CD127

Abbreviations: CTLA-4: cytotoxic T-lymphocyte antigen 4; DC: dendritic cell; FOXP3: forkhead/winged helix transcription factor; GITR: glucocorticoid-induced TNF receptor family-regulated gene; HBV: hepatitis B virus; HCC: hepatocellular carcinoma; HCV: hepatitis C virus; IL-T4: immunoglobulin-like transcript 4; LAG-3: lymphocyte-activation gene 3; PBMC: peripheral blood mononuclear cell; PD-1: programmed cell death 1; PD-L1: programmed cell death 1 ligand 1; RFA: radiofrequency ablation; RT-PCR: reverse transcription polymerase chain reaction; Tr1: type-1 regulatory T cells; Tregs: regulatory T cells

Additional Supporting Information may be found in the online version of this article.

Grant sponsors: Grant-In-Aid for Scientific Research from the Ministry of Education, Culture, Sports, Science and Technology of Japan, a Grant-in-Aid from the Ministry of Health, Labour and Welfare of Japan

DOI: 10.1002/ijc.27535

History: Received 23 Jul 2011; Accepted 28 Feb 2012; Online 15 Mar 2012

Correspondence to: Tatsuya Kanto, Department of Gastroenterology and Hepatology, Osaka University Graduate School of Medicine, 2-2 Yamadaoka, Suita 565-0871 Japan, Tel: +81-6-6879-3621, Fax: +81-6-6879-3629, E-mail: kantot@gh.med.osaka-u.ac.jp

Table 1. Clinical backgrounds of the patients enrolled in the study[1]

	HV	CH (C)	LC (C)	HCC (C)	HCC (B)	HCC (NBNC)
N	57	66	39	79	12	15
Gender (M/F)	35/22	44/22	23/16	44/35	8/4	9/6
Age (years)	56 ± 11	56 ± 18	61 ± 9	66 ± 11	56 ± 9	62 ± 13
ALT (IU/l)	ND	70 ± 15	44 ± 13	56 ± 17	65 ± 7	45 ± 11
Platelets ($10^4/\mu l$)	ND	15 ± 4	11 ± 4	12 ± 4	13 ± 4	12 ± 4
Total bilirubin (mg/ml)	ND	0.9 ± 0.4	1.6 ± 0.4[2]	0.9 ± 0.3	0.6 ± 0.1	0.7 ± 0.3
Alb (g/dl)	ND	3.7 ± 0.5	3.3 ± 0.4	3.1 ± 0.6[2]	3.5 ± 0.2	3.6 ± 0.3
AFP (ng/ml)[3]	ND	2-115 (15)	2-347 (16)	4-33357 (43)	7-12 (10)	10-16520 (23)
TNM stage[4] (I + II/III + IV)	–	–	–	55/24	9/3	9/6

[1]All values except for AFP are expressed as mean ± standard deviation. [2]$p < 0.05$ *vs.* CH (C) group. [3]Values are expressed as range (median).
[4]Seventh edition of International Union Against Cancer TNM staging system of HCC.
Abbreviations: HV, healthy volunteers; CH (C), LC (C), HCC (C), HCV-positive chronic hepatitis, liver cirrhosis and hepatocellular carcinoma; HCC (B), HBV-positive hepatocellular carcinoma; HCC (NBNC), non-B, non-C hepatocellular carcinoma; ALT, alanine aminotransferase; Alb, albumin; AFP, alfa-fetoprotein; ND, not determined.

periphery and are endowed with the ability to suppress antigen-specific T cells.[5] Several reports have shown that natural Tregs are increased in peripheral blood and/or tumor in patients with various types of cancer.[6] In HBV-infected HCC patients, an increase in natural Tregs and their suppressor functions against antigen-specific CTLs has been reported.[7] A correlation has been observed between natural Treg frequency and recurrence-free or overall survival of HCC patients.[8] However, it is yet to be determined if a distinct Treg subset is involved or not in the development of HCC.

The forkhead/winged helix transcription factor, FOXP3, is acknowledged as a major and specific marker of Tregs, the cellular expression of which is correlated with suppressive activities.[9] However, in the differentiation from naive T cells to effector/memory T cells, FOXP3 is transiently expressed but not sustained, suggesting that some proportion of $FOXP3^+$ T cells are not regulatory but activated ones.[10] These observations suggest that using FOXP3 as a marker of functionally regulatory cells would be limited and not suitable for adaptive Tregs. In recent studies, the expression of IL-7 receptor alpha chain (CD127) was found to be downregulated in Tregs and CD127 expression to be inversely correlated with FOXP3 expression.[11,12] Moreover, CD127-negative T cells are endowed with suppressive ability irrespective of their CD25 expression.[13] Alternatively, several studies have shown that CD127 is downregulated on $FOXP3^-$ Tr1 cells.[14,15] Due to the lack of specific or appropriate markers for identification of adaptive Tregs, it is yet to be confirmed that $FOXP3^-$ T cells are adaptive Tregs. Furthermore, little is known about the precise roles of $FOXP3^-$ regulatory cells in the development of HCC.

In this study, we focused on $FOXP3^-$ Tregs and tried to elucidate whether or not such cells are associated with the presence of HCC. To assess the feasibility of $FOXP3^-$ cells as a therapeutic target for immunological control of HCC, we tried to clarify the molecular mechanisms of its induction.

Material and Methods

Subjects

Among chronically HCV-infected patients who had been followed at Osaka University Hospital, we enrolled 184 patients who were further categorized into three groups according to the stages of liver disease: chronic hepatitis (CH), liver cirrhosis (LC) and HCC groups. The clinical stage of HCC was determined according to the TNM classification system of the International Union against Cancer (seventh edition). The study protocol was approved by the ethical committee at the Osaka University Graduate School of Medicine. At enrollment, written informed consent was obtained from all patients and volunteers. Some of HCC patients in this study received radiofrequency ablation (RFA) therapy. Indication for RFA therapy was based on therapeutic guidelines for HCC promoted by the Japan Society of Hepatology.[16] After the RFA session, the efficacy of tumor ablation or HCC recurrence thereafter was evaluated by computed tomography or magnetic resonance imaging scanning. In some of the HCC patients who underwent surgical resection, cancerous and adjacent noncancerous tissues were obtained at operation for further Treg analyses. As controls, 57 healthy subjects (HS) without history of liver diseases, 27 HCC patients with HBV infection (HBV–HCC group), those without HBV and HCV (non-B–, non-C [NBNC]–HCC group). The clinical backgrounds of the subjects are shown in Table 1.

Frequency analyses of peripheral and liver-infiltrating Tregs

Peripheral blood mononuclear cells (PBMCs) were stained with a combination of various fluorescence-labeled anti-human mouse or rat monoclonal antibodies (mAbs) as reported previously (17). The mAbs for CD4, CD25, CD127, FOXP3 and IL-10 were purchased from Becton Dickinson Biosciences (San Jose, CA). Fresh liver specimens were

washed twice with phosphate-buffered saline and were diced into 0.5 mm pieces. After these pieces were passed through a nylon mesh, liver-infiltrating lymphocytes were isolated by Ficoll-Hypaque density gradient centrifugation. These cells were stained with fluorescence-labeled Abs as performed for PBMC. For the analyses of FOXP3 and IL-10, we performed intracellular staining using a human FOXP3 staining kit (BD Biosciences) according to the manufacturer's instructions. The stained cells from PBMC or liver were analyzed by FACS Canto (BD Biosciences) and Cell Quest software.

Functional analysis of regulatory T cell subsets

To obtain live Tregs for functional analyses, we collected four populations of $CD4^+$ T cells according to the patterns of CD25 and CD127 expressions by FACS Aria (BD Biosciences). We cocultured various numbers of sorted cells with 1×10^5 allogenic naive $CD4^+CD25^-$ T cells in the presence of agonistic anti-CD3 and anti-CD28 Abs (BD Biosciences Pharmingen) on 96-well flat-bottom plates (Corning, Corning, NY) for 5 days. The proliferation of cells was assessed by incorporation of [3H]-thymidine. To clarify the suppression mechanism by Tregs, the cells were cultured with or without separation by transwell inserts (pore size 0.4 μm, Corning). Alternatively in some experiments, the cells were cultured in the presence or absence of neutralizing 10 ng/ml anti-IL-10 or anti-TGF-β Abs (R&D Systems, Mckinley, MN) or isotype IgG.

To examine regulatory cells possess suppressive function on recall antigen-specific $CD4^+$ T cell responses, we cocultured 1×10^4 each of sorted cells from some HCC patients with 1×10^5 autologous $CD4^+$ T cells in the presence or absence of 20 μg/ml of tetanus toxoid (Sigma) for 5 days, stimulated with 10 IU/ml of recombinant human IL-2 (BD Pharmingen). The proliferation of cells was assessed using WST-8 (2-(2-methoxy-4-nitrophenyl)-3-(4-nitrophenyl) -5 -(2,4-disulfophenyl)-2H-tetrazolium, monosodium salt) reagent in the Cell Counting Kit-8 (Dojindo, Japan) according to the manufacturer's instructions.

Real-time RT-PCR

To analyze gene profiles of Tregs, we collected $CD4^+CD25^{high+}CD127^-$ and $CD4^+CD25^-CD127^-$ T cells using FACS Aria. Extraction of total RNA and subsequent real-time reverse transcription polymerase chain reaction (RT-PCR) was performed as reported previously with some modifications.[17] Assays-on-demand primers and probes (Applied Biosystems, Foster City, CA) were used to quantify FOXP3, cytotoxic T-lymphocyte antigen 4 (CTLA-4), glucocorticoid-induced TNF receptor family-regulated gene (GITR), lymphocyte-activation gene 3 (LAG3), IL-21, programmed cell death 1 (PD-1) and c-masculoaponeurotic fibrosarcoma (c-Maf) expression. The expressions of molecules were given as the relative values to the calibrator samples. To standardize the amount of total RNA, we quantified β-actin mRNA from each sample as a control of internal RNA and corrected all values with this.

Induction of $CD4^+CD25^-CD127^-FOXP3^-$ T cells from PBMC

To clarify the molecular mechanisms of Treg induction, we cultured 1×10^6 naive $CD4^+CD25^-$T cells with 1×10^5 autologous monocyte-derived dendritic cells (DCs) and mitomycin C (Sigma-Aldrich, St. Louis, MO)-treated 1×10^5 HCC cell lines, Huh7 or HepG2 (AmericanType Culture Collection, Manassas, VA) on 24-well flat-bottom plates for 5 days. Monocyte-derived DCs were generated from $CD14^+$ cells as reported previously.[18] On days 2 and 4 of the coculture, recombinant human IL-2 (10 IU/ml), IL-10 (20 IU/ml) and IL-15 (20 IU/ml; BD Pharmingen) were added to the cells. On day 6, they were stimulated with phorbol 12-myristate 13 acetate (PMA; 1 ng/ml) and ionomycin (1 μmol/l) in the presence of anti-CD3 mAb (1 μg/ml) and breferdin A (1 μg/ml) (BD Pharmingen). In some experiments, we separated relevant cells by transwell inserts (pore size 0.4 μm) or added 10 μg/ml neutralizing Abs against TGF-β (R&D), HLA-DR (BD), PD-1 (R&D), programmed cell death 1 ligand 1 (PD-L1; e-Bioscience) or immunoglobulin-like transcript 4 (IL-T4) (e-Bioscience) during the culture. Subsequently, the cells were stained with Abs for CD4, CD25, CD127, FOXP3 and IL-10 and then were subjected to FACS analysis.

Knockdown of PD-L1 and HLA-G genes in HCC cell lines by siRNA

To confirm the molecules involving Treg induction, we knocked down PD-L1 and HLA-G genes in Huh7 cells by means of RNA interference. We used the small interfering RNA (siRNA) cocktail targeting human CD274 (PD-L1) or human leukocyte antigen G (HLA-G), provided by COSMO BIO (Tokyo, Japan). Transfection of siRNA to Huh7 or HepG2 cells was performed using lipofectamine RNAiMAX (Invitrogen) according to the manufacturer's instructions. To assess the efficiency of transfection, we compared the mRNA expression of target genes before and after the procedure by real time RT-PCR.

Statistical analyses

The Jonckheere-Terpstra test was used for the analysis of dose-dependent tendency. The Mann-Whitney nonparametric *U* test was used to compare differences in unpaired samples and Kruskal–Wallis nonparametric tests were used to compare differences among multiple groups, respectively. Friedman test with Bonferroni multiple comparison tests was used to compare differences in paired samples. All tests were two-tailed, and a $p < 0.05$ was considered statistically significant.

Results

$CD4^+$ T cells with distinct patterns of CD127 and FOXP3 expression were identified

According to the expression of CD25 and CD127 in $CD4^+$ T cells, we separated them into four groups: $CD25^{high+}CD127^-$, $CD25^-CD127^-$, $CD25^{high+}CD127^+$ and $CD25^-CD127^+$ cells, respectively (Fig. 1*a*). Most of the $CD4^+CD25^{high+}CD127^-$

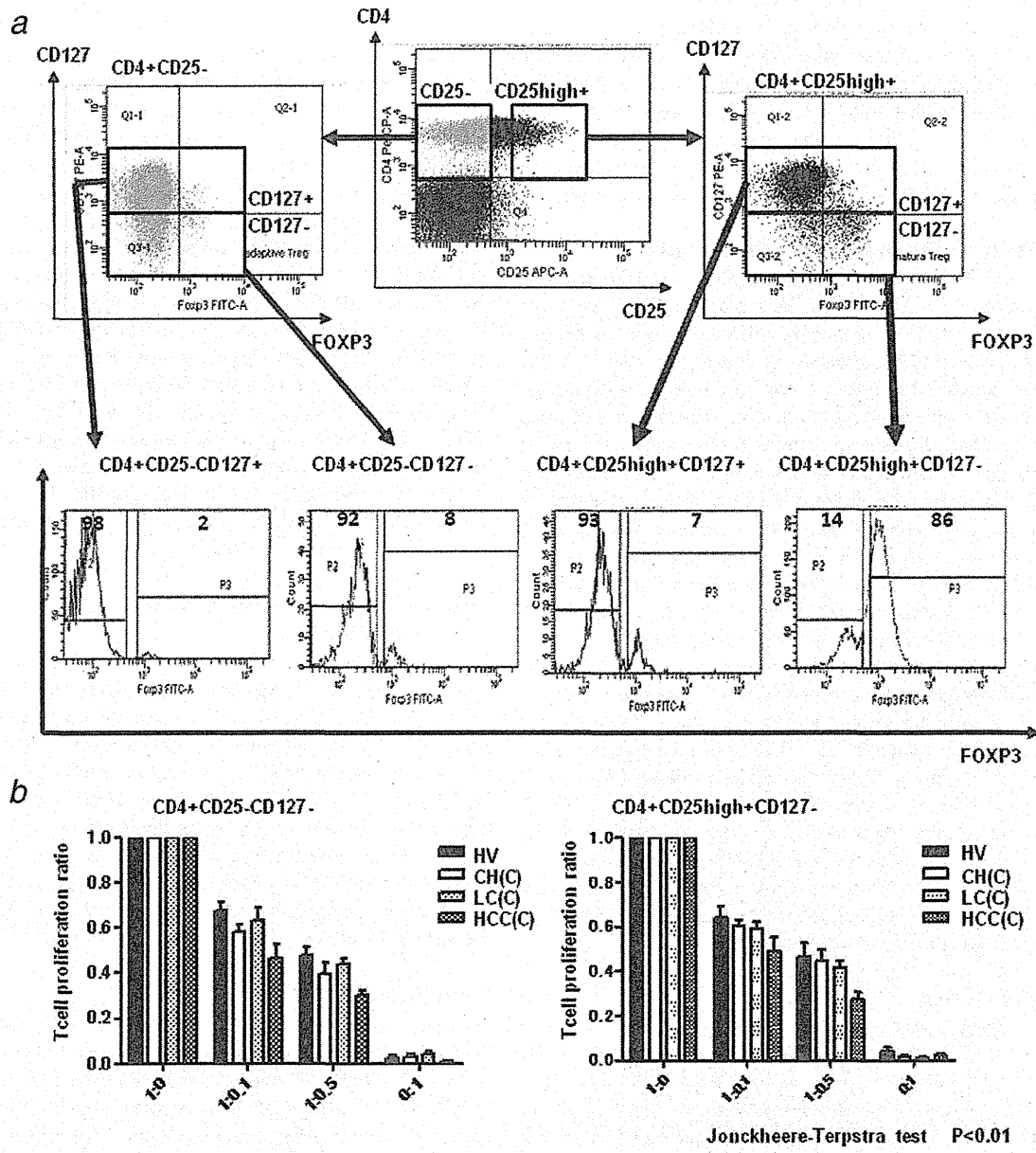

Figure 1. $CD4^+CD25^-CD127^-$ and $CD4^+CD25^{high+}CD127^-$ T cells are Tregs. (*a*) $CD4^+$ T cells are separated into four subpopulations: $CD4^+CD25^{high+}CD127^+$, $CD4^+CD25^{high+}CD127^-$, $CD4^+CD25^-CD127^+$ and $CD4^+CD25^-CD127^-$ cells, respectively. These cells were examined for FOXP3 expression. The numbers in the histograms depict the percentages of gated cells. Representative plots from three patients and donors are shown. (*b*) Sorted $CD4^+CD25^-CD127^-$ T cells and $CD4^+CD25^{high+}CD127^-$ T cells obtained from patients and healthy donors were added at various ratios to allogenic $CD4^+$ T cells stimulated with anti-CD3 and anti-CD28 Abs. After 5 days of culture, $CD4^+$ T cell proliferation was evaluated by incorporation of ^{3}H-thymidine. The bars indicate the ratio of counts per minutes (cpm) in various responders to regulatory cells ratio to those at 1:0. The results are shown as mean + SEM of ten patients or donors in each group. The dose dependency was analyzed by Jonckheere Terpstra test and comparison among the disease statuses was analyzed by Wilcoxon rank sum test with Bonferroni multiple comparison test. HV, healthy volunteers; CH(C), LC(C), HCC (C), HCV-infected chronic hepatitis, liver cirrhosis or hepatocellular carcinoma, respectively.

cells express FOXP3 (>80%). In contrast, the populations of $CD4^+CD25^-CD127^-$, $CD4^+CD25^{high+}CD127^+$ and $CD4^+CD25^-CD127^+$ lack FOXP3 expression (<10%). These results show that, except for $CD4^+CD25^{high+}CD127^-$ cells, the remaining $CD127^-$ cells lack FOXP3 and CD25 expression ($CD4^+CD25^-CD127^-FOXP3^-$).

$CD4^+CD25^{high+}CD127^-$ cells and $CD4^+CD25^-CD127^-$ T cells are suppressors against allogeneic T cells with distinct mechanisms

To examine which cell populations exert a suppressive capacity, we added each phenotype of cells separated from the subjects to allogeneic $CD4^+$ T cells. The sorted $CD4^+CD127^+$ T cells had no regulatory activities regardless of CD25 expression (data not shown). In contrast, $CD127^-$ cells, either $CD25^-$ or $CD25^{high+}$, significantly inhibited allogenic $CD4^+$ T cell proliferation in a dose-dependent manner, at comparable levels (Fig. 1*b*). Of note is that their suppressive capacity did not differ at the single cell level between patients and donors, regardless of the stage of liver disease (Fig. 1*b*). In addition, $CD127^-$ cells are anergic irrespective of CD25 expression (Fig. 1*b*). The suppressive ability of $CD4^+CD25^{high+}CD127^-$ cells was significantly abrogated by transwells and anti-TGF-β Ab, suggesting that they work in cell–cell contact-dependent and TGF-β-dependent manners (Supporting Information Fig. 1). By contrast, suppression by $CD4^+CD25^-CD127^-$ cells was alleviated by anti-IL-10 Ab but not by transwells, showing that they are contact-independent but IL-10-dependent (Supporting Information Fig. 1). These results show that $CD4^+CD25^-CD127^-$ cells possess a suppressive capacity with distinct machinery from $CD4^+CD25^{high+}CD127^-$ cells. In the setting of tetanus toxoid-reactive $CD4^+$ T cell response, each type of cells tended to be comparably suppressive (Supporting Information Fig. 2).

$CD4^+CD25^{high+}CD127^-$ and $CD4^+CD25^-CD127^-$ T cells display distinct gene profiles

$CD4^+CD25^{high+}CD127^-$ and $CD4^+CD25^-CD127^-$ T cells were sorted by FACS Aria and were subjected to real-time RT-PCR analyses. The expressions of FOXP3, CTLA-4 and GITR in $CD4^+CD25^{high+}CD127^-$ cells were higher than those in $CD4^+CD25^-CD127^-$ T cells, while those of LAG-3, IL-21, PD-1 and c-Maf in $CD4^+CD25^-CD127^-$ T cells were higher than those in $CD4^+CD25^{high+}CD127^-$ cells, respectively (Fig. 2). Thus, these two types of regulatory cells have distinct molecular profiles. As we described in the previous sections, $CD4^+CD25^-CD127^-$ cells with regulatory capacity lack FOXP3 expression (Figs. 1 and 2). Thus, we tentatively defined such cells as $CD25^-FOXP3^-$ Tregs in the following parts.

$CD25^-FOXP3^-$ Tregs are increased in HCC patients and their increments are associated with cancer progression

We compared the frequency of Treg subsets among healthy donors and HCV-infected patients. In HCC patients, $CD25^-FOXP3^-$ Tregs or $CD4^+$ $CD127^-$ $CD25^{high+}$ $FOXP3^+$ cells ($CD25^{high+}FOXP3^+$ Tregs) frequency in the periphery was significantly higher than those in other groups (Fig. 3*a*). The frequency of each type of Tregs is not correlated with HCV quantity (Supporting Information Fig. 3). These results show that the increase in $CD25^-FOXP3^-$ or $CD25^{high+}FOXP3^+$ Tregs is correlated with the development of liver cancer, but not with HCVRNA titers. Such increment of peripheral Tregs is also observed in HBV-HCC or NBNC-HCC patients (Fig. 3*a*).

Next, we compared the frequency of Tregs between PBMC and liver-infiltrating lymphocytes in HCC patients. Both $CD25^-FOXP3^-$ and $CD25^{high+}FOXP3^+$ Tregs are detected in liver-infiltrating lymphocytes, and $CD25^-FOXP3^-$ Tregs are higher in tumor-infiltrating lymphocytes than those in nontumor-infiltrating and circulating lymphocytes (Fig. 3*b*). These results demonstrate that $CD25^-FOXP3^-$ Tregs increase both in the liver and in the periphery in parallel with the development of cancer.

We serially examined the frequency of $CD25^-FOXP3^-$ Tregs and $CD25^{high+}FOXP3^+$ Tregs before and after RFA therapy. The $CD25^-FOXP3^-$ Tregs frequency dramatically decreased after successful HCC ablation and further subsided in patients without intrahepatic recurrence (Fig. 4*a*). In clear contrast, in patients with subsequent HCC recurrence, $CD25^-FOXP3^-$ Tregs increased before apparent radiological identification of HCC (Fig. 4*a*). Such dynamic frequency changes in parallel with HCC recurrence were not apparent in $CD25^{high+}FOXP3^+$ Tregs (Fig. 4*b*). Therefore, $CD25^-FOXP3^-$ Treg frequency is more closely correlated than $CD25^{high+}FOXP3^+$ Tregs with the presence or absence of HCC.

PD-L1, IL-T4 and HLA-G are involved in the induction of $CD4^+CD25^-CD127^-FOXP3^-$ IL-10^+ T cells

After the culture of naive $CD4^+$ T cells, DC and Huh7 or HepG2, we found that $CD4^+CD25^-CD127^-FOXP3^-$ cells produce IL-10 (Fig. 5*a*), whereas $CD4^+CD25^+CD127^-FOXP3^+$ cells do not (Supporting Information Fig. 4). Since $CD4^+CD25^-CD127^-$ cells use IL-10 as one of suppressor mechanisms (Supporting Information Fig. 1), such IL-10^+ $CD4^+CD25^-CD127^-FOXP3^-$ T cells are functionally competent $CD25^-FOXP3^-$ Tregs (Fig. 5*a*). In culture, the frequency of IL10^+ $CD25^-FOXP3^-$ T cells decrease in the presence of anti-TGF-β, anti-PD-1, anti-PD-L1 or anti-ILT4 Abs, with the difference being the most significant with anti-PD-L1 or anti-ILT4 Abs (Fig. 5*b*). Next, in the absence of DC or the separation of T cells from HCC cell lines significantly reduced IL10^+ $CD25^-FOXP3^-$ T cell induction, whereas separation of T cells from DC did not change it (Fig. 5*c*). These results indicate that the contact between T cells and HCC cell lines is indispensable for IL-10^+ $CD25^-FOXP3^-$ T cell induction, but the contacts between T cells and DC or between DC and HCC cell lines are not, respectively. Similarly, the addition of anti-PDL1 or anti-IL-T4 Abs to this culture resulted in suppression of IL-10^+ $CD25^-FOXP3^-$ T cell induction, regardless of the presence of transwells (Fig. 5*c*).

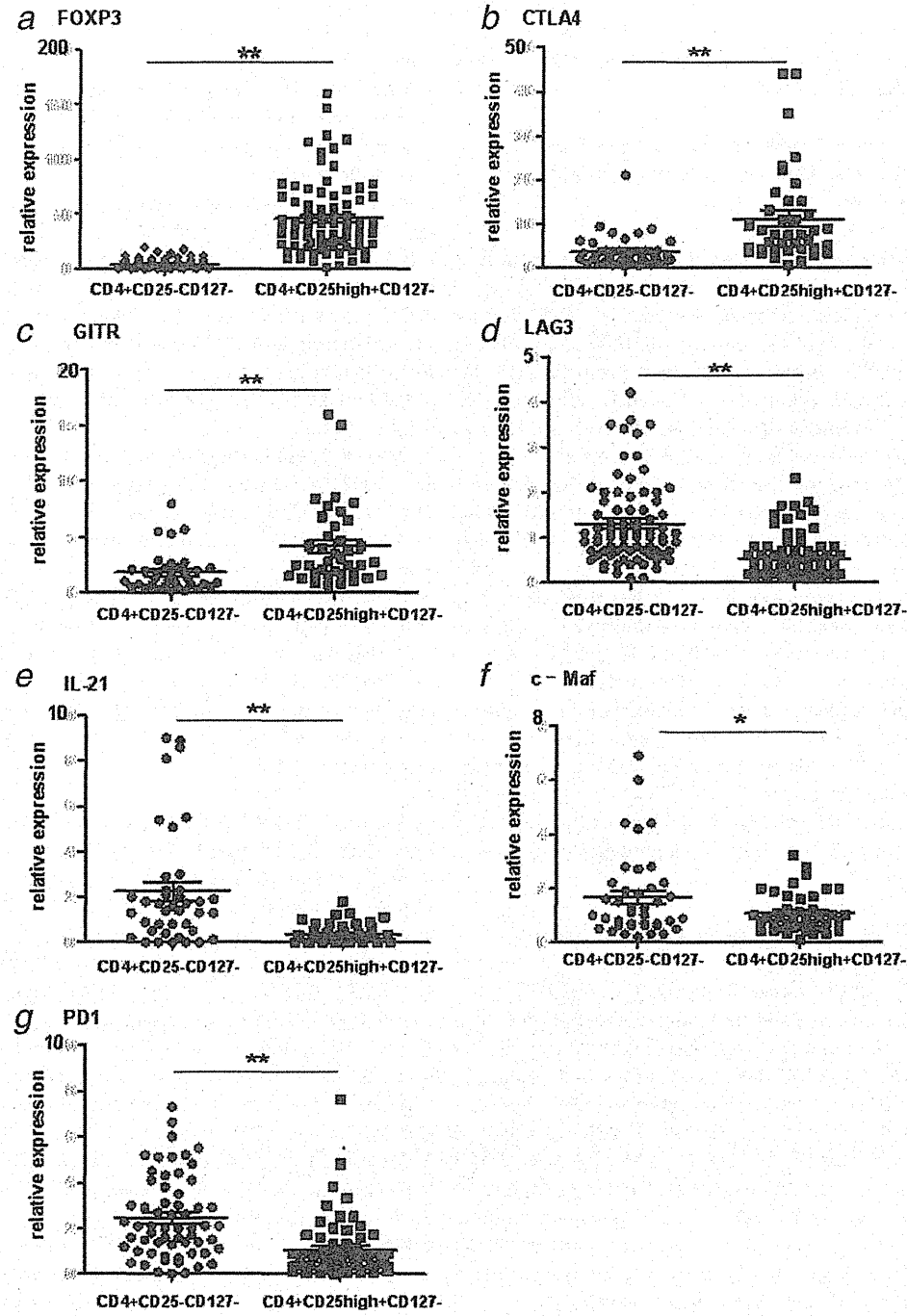

Figure 2. $CD4^+CD25^-CD127^-$ T cells and $CD4^+CD25^{high+}CD127^-$ T cells display distinct gene profiles. Sorted $CD4^+CD25^-CD127^-$ cells and $CD4^+CD25^{high+}CD127^-$ cells from PBMC of HCC patients were subjected to real-time RT-PCR for the analyses of FOXP3 (*a*), CTLA4 (*b*), GITR (*c*), LAG3 (*d*), IL-21 (*e*), c-Maf (*f*) and PD1 (*g*). The results are shown in relative expression of relevant genes to those of β-actin. *: $p < 0.05$; **: $p < 0.01$ by Mann-Whitney *U* test with Welch's correction.

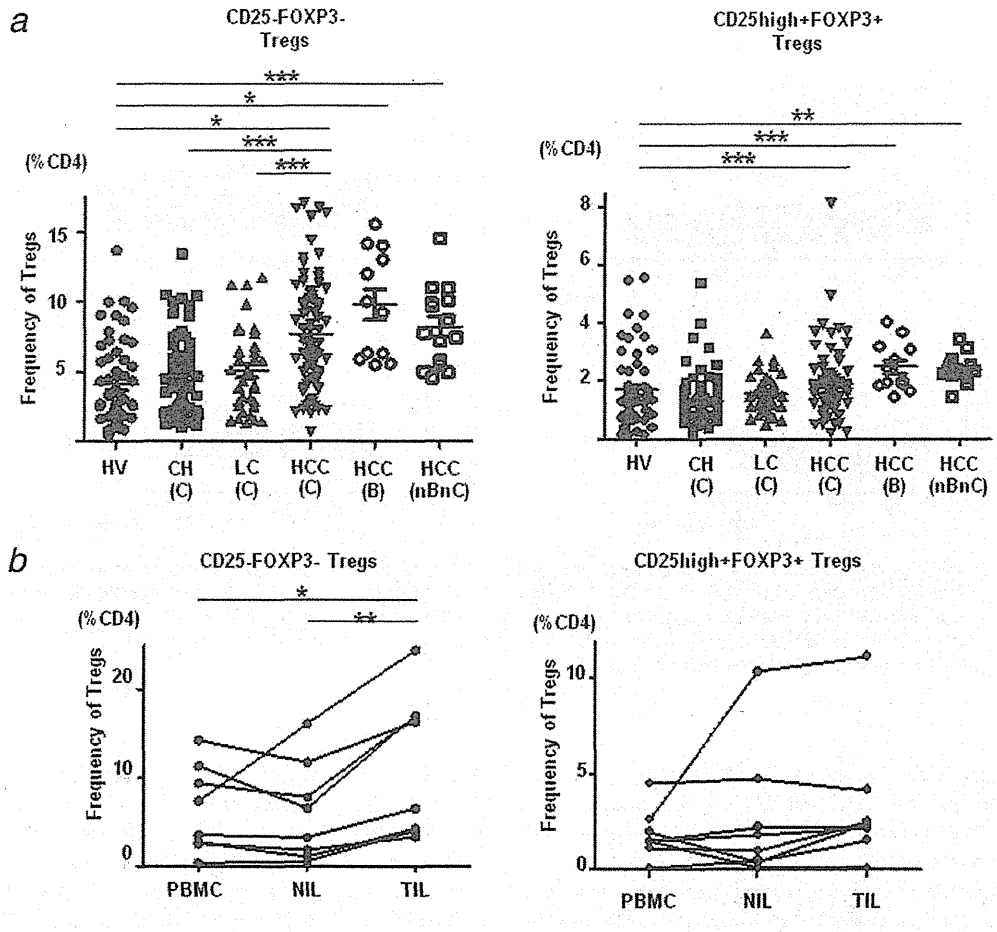

Figure 3. $CD25^{-}FOXP3^{-}$ Tregs and $CD25^{high+}FOXP3^{+}$ Tregs increase in HCC patients both in the periphery and in the liver. (*a*) The frequencies of $CD25^{-}FOXP3^{-}$ Tregs ($CD4^{+}CD25^{-}CD127^{-}$ $FOXP3^{-}$) and $CD25^{high+}FOXP3^{+}$ Tregs ($CD4^{+}CD25^{high+}CD127^{-}FOXP3^{+}$) in $CD4^{+}$ T cells were compared among the groups. HV, healthy volunteers; CH(C), LC(C), HCC (C), HCV-infected chronic hepatitis, liver cirrhosis or hepatocellular carcinoma, respectively; HCC (B), HBV-positive; HCC (nBnC), HCV-negative and HBV-negative HCC patients. The horizontal bars indicate mean ± standard deviation. *: $p < 0.05$; **: $p < 0.01$; ***: $p < 0.001$ by Kruskal–Wallis test with Dunn's multiple comparison test. (*b*) $CD25^{-}FOXP3^{-}$ Tregs and $CD25^{high+}FOXP3^{+}$ Tregs are present in tumor-infiltrating lymphocytes of HCC patients. Lymphocytes from HCC, nontumor liver tissue and PBMC were collected from identical nine HCC patients, and the frequency of $CD25^{-}FOXP3^{-}$ Tregs and $CD25^{high+}FOXP3^{+}$ Tregs in them was compared. PBMC, peripheral blood mononuclear cells; NIL, nontumor tissue infiltrating lymphocytes; TIL, tumor-infiltrating lymphocytes. *: $p < 0.05$; **: $p < 0.01$, by Friedman test with Bonferroni multiple comparison test.

IL-T4 is expressed on DC and transmits inhibitory signals after ligation with HLA-G. To confirm that the HLA-G and PD-L1 expressed in HCC are responsible for $IL10^{+}$ $CD25^{-}FOXP3^{-}$ T cell induction, we knocked down HLA-G and/or PD-L1 in Huh7 cells by siRNA and subjected them to the abovementioned *in vitro* cultures (Fig. 5*d*). As a result, $IL10^{+}$ $CD25^{-}FOXP3^{-}$ T cell frequency is significantly decreased in the presence of siRNA-treated HCC, but not with mock-transfected HCC (Fig. 5*e*). These results demonstrate that DC and HCC cells are actively involved in $IL\text{-}10^{+}$ $CD25^{-}FOXP3^{-}$ T cell induction, in which PD-L1, IL-T4 and HLA-G are indispensible.

Discussion

In this study, we focused on $CD25^{-}FOXP3^{-}$ Tregs in HCC patients, which are distinct from $CD25^{high+}FOXP3^{+}$ natural Tregs in cellular phenotypes, genetic profiles and functional aspects. We demonstrated that; (*i*) $CD4^{+}CD127^{-}CD25^{-}$ cells (as defined as $CD25^{-}FOXP3^{-}$ cells in this study) are endowed with suppressive capacity comparably with

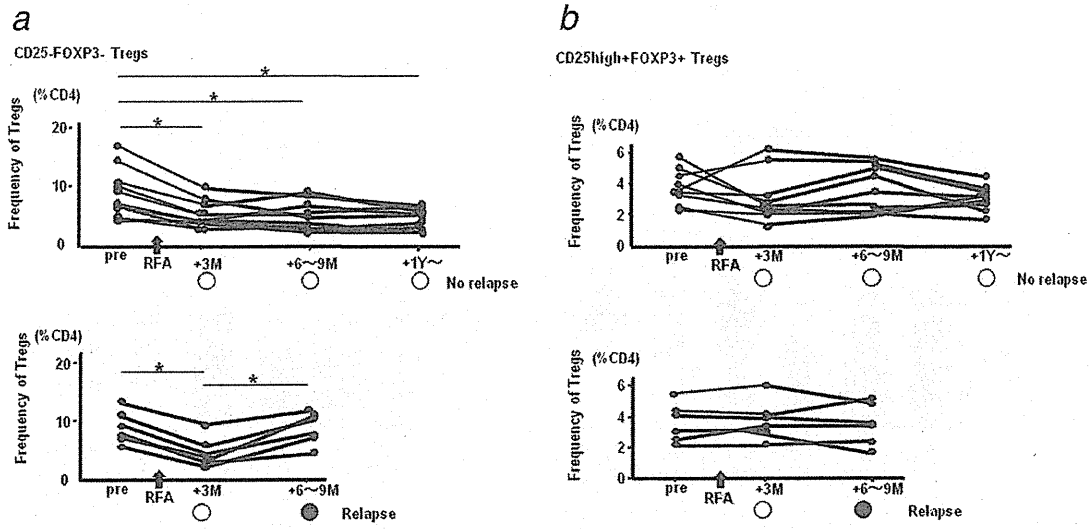

Figure 4. CD25$^-$FOXP3$^-$ Tregs increase in parallel with post therapeutic HCC recurrence. In HCC patients who underwent RFA therapy, frequencies of CD25$^-$FOXP3$^-$ Tregs (*a*) and CD25^{high+}FOXP3$^+$ Tregs (*b*) in CD4$^+$ T cells are examined serially before RFA sessions and after confirmation of complete ablation of relevant HCC lesions. Open circles (○)depict the time points without HCC recurrence under CT/MRI examinations and closed circles (●)are those with detectable HCC recurrence, respectively. Arrows indicate the time points of RFA sessions. *: $p < 0.05$ by Friedman test with Bonferroni multiple comparison test.

CD4$^+$CD127$^-$CD25^{high+} cells (CD25^{high+}FOXP3$^+$ cells) and (*ii*) the frequency of CD25$^-$FOXP3$^-$ Tregs changes more dynamically than those of CD25^{high+}FOXP3$^+$ Tregs in correlation with post-therapeutic HCC recurrence.

Extensive studies have been carried out on the role of natural Tregs in cancer patients, of which are conventionally defined as CD25^{high+}FOXP3$^+$ T cells. Pharmaceutical deprivation of CD25$^+$ T cells *in vivo* were tried to improve immune reactivity against cancers; however, most of the study results were unsatisfactory.[19,20] Such experiences raise the possibility that the involvement of CD25$^-$ Tregs in the pathogenesis of certain cancers. In support for this, the existence of CD25$^-$FOXP3$^-$ Tregs has been reported in mice and human, in relation to viral infection or cancers.[21–23] The comparative roles of CD25^{high+}FOXP3$^+$ natural Tregs and CD25$^-$ Tregs in human diseases are still largely unknown. It is reported that CD127 expression is inversely correlated with a FOXP3 and CD127 negative population broadly encompassing regulatory cells.[11,12] Several investigators reported that CD127 expression on T cells is aberrantly regulated with regard to their functional relevance.[24,25] Taking these findings into consideration, we aimed to identify distinct type of Tregs in CD4$^+$CD127$^-$ population. Consequently, we found a functional regulatory subset in CD4$^+$CD25$^-$CD127$^-$ T cells, which differ from CD4$^+$CD25^{high+}CD127$^-$ Tregs in molecular profiles and inhibitory mechanisms. The profile of CD4$^+$CD25$^-$CD127$^-$ T cells is quite unique; they express more LAG-3, IL-21, c-Maf and PD-1 but less FOXP3, CTLA-4 and GITR than CD4$^+$CD25^{high+}CD127$^-$ Tregs do. In support of our results, Pot *et al.* reported that IL-27 induces IL-21 and c-Maf, which are critically involved in the differentiation of IL-10-producing Tr1.[26] As for functional aspects, we showed that CD4$^+$CD25$^-$CD127$^-$ cells use IL-10 as suppressive machineries, not completely but in part. Based on these characteristics, it is likely that CD4$^+$CD25$^-$CD127$^-$FOXP3$^-$ cells, as defined as CD25$^-$FOXP3$^-$ Tregs in this study, are presumed to be aforementioned Tr1 cells. Such phenotype of T cells are compatible with Tr1-like cells in human, as reported by Haringer *et al.*[14] To confirm that, several additional examinations, such as antigen-specific suppressive capacity, need to be carried out. Using tetanus toxoid as a representative of general recall antigens in this study, CD4$^+$CD25$^-$CD127$^-$ cells and CD4$^+$CD25high$^+$CD127$^-$ cells tended to be suppressive on autologous CD4$^+$ T cell proliferation (Supporting Information Fig. 2). Further analysis needs to be performed on this issue, using other sets of recall antigens.

To therapeutically control Tregs *in vivo*, extensive studies have been carried out to disclose the mechanisms of the induction or attraction of FOXP3$^+$ Tregs.[27,28] Likewise, it is tempting to consider that CD25$^-$FOXP3$^-$ Tregs depletion would have a favorable impact on the clinical features of the patients. Thus, identifying the molecules involved in CD25$^-$FOXP3$^-$, Treg induction should be carried out for the future development of Treg-oriented therapeutic approach. For this purpose, we successfully expanded CD4$^+$CD25$^-$CD127$^-$FOXP3$^-$IL10$^+$ cells from naive CD4$^+$CD25$^-$T cells. Such cultured cells contained approximately 10% of IL-10$^+$ cells, which subsequently

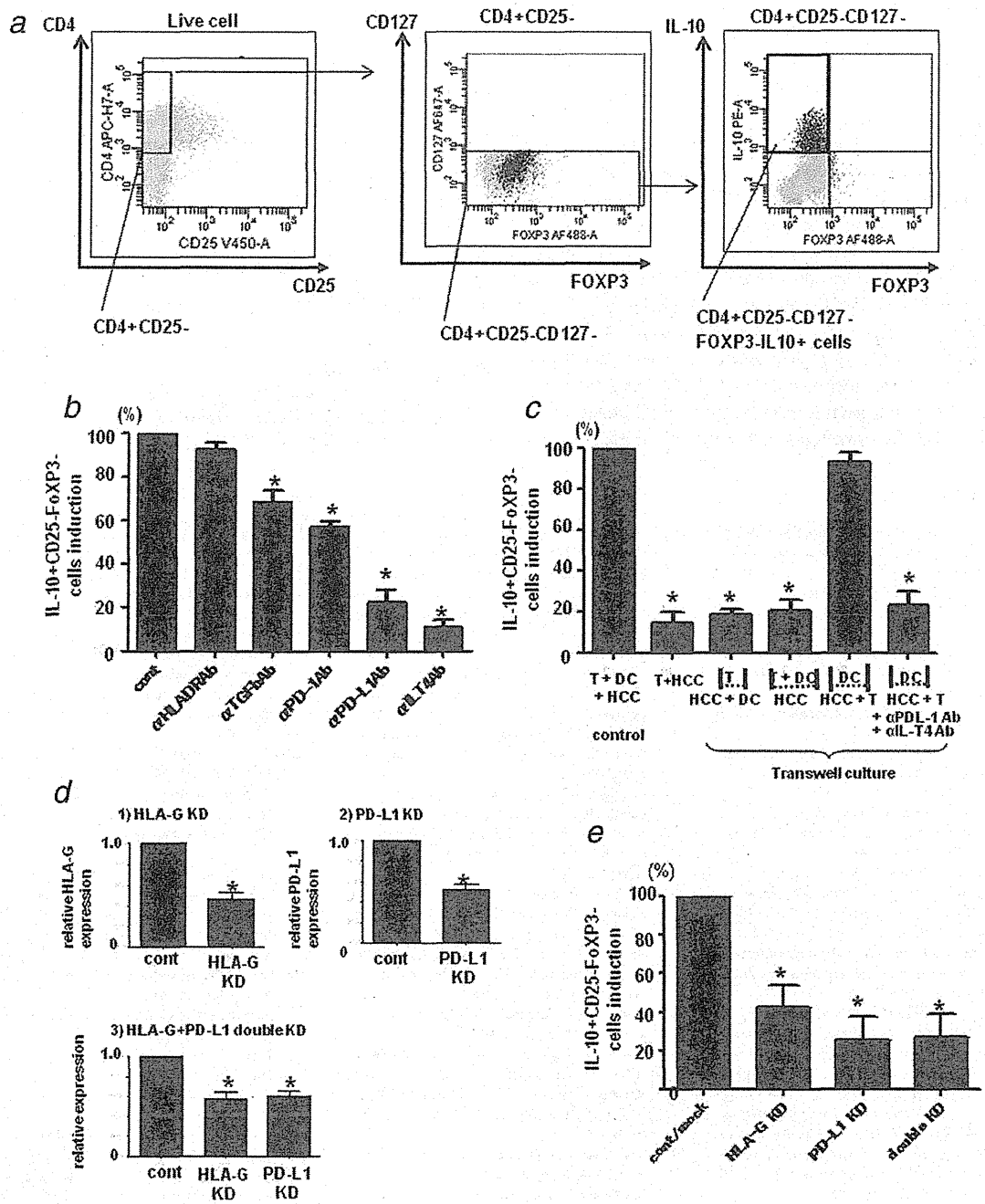

Figure 5. HLA-G and PD-L1 in HCC and IL-T4 in DC are involved in the induction of IL-10$^+$CD25$^-$FOXP3$^-$ Tregs. After culture of CD4$^+$CD45RA$^+$ naive T cells with autologous monocyte-derived dendritic cells and Huh-7 or HepG2, CD4$^+$ CD127$^-$ CD25$^-$FOXP3$^-$IL-10$^+$ T cells (IL-10$^+$CD25$^-$FOXP3$^-$ Tregs) were generated. (*a*) Representative dot plots from results of seven healthy volunteers are shown. In the abovementioned coculture system, various neutralizing/masking Abs (*b*) or transwell inserts (*c*) were added and the results were compared with the frequencies of IL-10$^+$CD25$^-$FOXP3$^-$ Tregs with or without treatments. In addition, we transfected siRNA against HLA-G and/or PD-L1 to Huh-7 and cocultured them with naive CD4$^+$ T cells and DC as the same as above. The efficiency of gene silencing was evaluated by the comparison of transcripts of HLA-G or PD-L1 with or without siRNA transfection (*d*). The frequency of IL-10$^+$CD25$^-$FOXP3$^-$ Tregs after the culture was compared with mock-transfected ones (*e*). In Figures 5-B, 5-C and 5-E, the bars indicate the ratio of IL-10$^+$CD25$^-$FOXP3$^-$ Tregs frequency (mean + standard deviation) between those with treatment and without from three series of experiments. *: $p < 0.05$ by Wilcoxon rank sum test.

tended to inhibit proliferation of allogeneic $CD4^+$ T cells (data not shown). Using this culture, we demonstrated that DCs are indispensible for IL-10^+ $CD25^-FOXP3^-$ Tregs induction *in vitro* by way of PD-1/PD-L1 and IL-T4/HLA-G pathways. Several reports showed that such molecular interactions are involved in the generation of regulatory cells in cancer patients.[29,30] In patients with HCC, a positive correlation is observed between the expression of PD-L1 or HLA-G in cancer tissue and the poorer prognosis of the patients,[31,32] suggesting that such molecules are involved in cancer development. As for HLA-G in this study, direct cellular contact between DC and HCC is not necessary in IL-10^+ $CD25^-FOXP3^-$ Tregs induction, suggesting that soluble HLA-G released from HCC may play an active role. In our hands, soluble HLA-G was measurable in culture supernatants of HCC cell lines and in serum samples from HCC patients (data not shown). Further investigation is arguably needed to elucidate whether soluble HLA-G is functional or not in HCC patients.

In summary, we demonstrate that $CD25^-FOXP3^-$ Tregs are increased in HCC patients, which change dynamically in response to HCC occurrence and post-therapeutic recurrence. Cross-talks among HCC cells, DC and $CD4^+$ T cells are required for IL-10^+ $CD25^-FOXP3^-$ Tregs induction, in which PD-L1, HLA-G and IL-T4 are critically involved. Although further investigation is needed to prove that deprivation or inactivation of $CD25^-FOXP3^-$ Tregs improves immune responses *in vivo*, such molecules could serve as targets of Treg-oriented therapeutic intervention for HCC.

Acknowledgements

The authors thank T Daimon, Department of Mathematics, Hyogo Medical University, for help with the statistical analysis; M. Hirose, Y. Kuronaka and H. Shimizu of the BD Laboratory for their technical assistance.

References

1. Parkin DM, Bray F, Ferlay J, Pisani P. Estimating the world cancer burden: globocan 2000. *Int J Cancer* 2001;94:153–6.
2. Bruix J, Sherman M. Management of hepatocellular carcinoma. *Hepatology* 2005;42: 1208–36.
3. Davila JA, Morgan RO, Shaib Y, McGlynn KA, El-Serag HB. Hepatitis C infection and the increasing incidence of hepatocellular carcinoma: a population-based study. *Gastroenterology* 2004; 127:1372–80.
4. Sakaguchi S, Yamaguchi T, Nomura T, Ono M. Regulatory T cells and immune tolerance. *Cell* 2008;133:775–87.
5. Jonuleit H, Schmitt E. The regulatory T cell family: distinct subsets and their interrelations. *J Immunol* 2003;171:6323–7.
6. Liyanage UK, Moore TT, Joo HG, Tanaka Y, Herrmann V, Doherty G, Drebin JA, Strasberg SM, Eberlein TJ, Goedegebuure PS, Linehan DC. Prevalence of regulatory T cells is increased in peripheral blood and tumor microenvironment of patients with pancreas or breast adenocarcinoma. *J Immunol* 2002;169:2756–61.
7. Ormandy LA, Hillemann T, Wedemeyer H, Manns MP, Greten TF, Korangy F. Increased populations of regulatory T cells in peripheral blood of patients with hepatocellular carcinoma. *Cancer Res* 2005;65:2457–64.
8. Fu J, Xu D, Liu Z, Shi M, Zhao P, Fu B, Zhang Z, Yang H, Zhang H, Zhou C, Yao J, Jin L, et al. Increased regulatory T cells correlate with CD8 T-cell impairment and poor survival in hepatocellular carcinoma patients. *Gastroenterology* 2007;132:2328–39.
9. Hori S, Nomura T, Sakaguchi S. Control of regulatory T cell development by the transcription factor Foxp3. *Science* 2003;299: 1057–61.
10. Ziegler SF. FOXP3: of mice and men. *Annu Rev Immunol* 2006;24:209–26.
11. Liu W, Putnam AL, Xu-Yu Z, Szot GL, Lee MR, Zhu S, Gottlieb PA, Kapranov P, Gingeras TR, Fazekas de St Groth B, Clayberger C, Soper DM, et al. CD127 expression inversely correlates with FoxP3 and suppressive function of human CD4+ T reg cells. *J Exp Med* 2006;203:1701–11.
12. Seddiki N, Santner-Nanan B, Martinson J, Zaunders J, Sasson S, Landay A, Solomon M, Selby W, Alexander SI, Nanan R, Kelleher A, Fazekas de St Groth B. Expression of interleukin (IL)-2 and IL-7 receptors discriminates between human regulatory and activated T cells. *J Exp Med* 2006;203:1693–700.
13. Hartigan-O'Connor DJ, Poon C, Sinclair E, McCune JM. Human CD4+ regulatory T cells express lower levels of the IL-7 receptor alpha chain (CD127), allowing consistent identification and sorting of live cells. *J Immunol Methods* 2007;319:41–52.
14. Haringer B, Lozza L, Steckel B, Geginat J. Identification and characterization of IL-10/IFN-gamma-producing effector-like T cells with regulatory function in human blood. *J Exp Med* 2009;206:1009–17.
15. Couper KN, Blount DG, Wilson MS, Hafalla JC, Belkaid Y, Kamanaka M, Flavell RA, de Souza JB, Riley EM. IL-10 from CD4CD25Foxp3CD127 adaptive regulatory T cells modulates parasite clearance and pathology during malaria infection. *PLoS Pathog* 2008;4:e1000004.
16. Arii S, Sata M, Sakamoto M, Shimada M, Kumada T, Shiina S, Yamashita T, Kokudo N, Tanaka M, Takayama T, Kudo M. Management of hepatocellular carcinoma: Report of Consensus Meeting in the 45th Annual Meeting of the Japan Society of Hepatology (2009). *Hepatol Res* 2010; 40:667–85.
17. Itose I, Kanto T, Kakita N, Takebe S, Inoue M, Higashitani K, Miyazaki M, Miyatake H, Sakakibara M, Hiramatsu N, Takehara T, Kasahara A, et al. Enhanced ability of regulatory T cells in chronic hepatitis C patients with persistently normal alanine aminotransferase levels than those with active hepatitis. *J Viral Hepat* 2009;16:844–52.
18. Kanto T, Hayashi N, Takehara T, Tatsumi T, Kuzushita N, Ito A, Sasaki Y, Kasahara A, Hori M. Impaired allostimulatory capacity of peripheral blood dendritic cells recovered from hepatitis C virus-infected individuals. *J Immunol* 1999;162:5584–91.
19. Mahnke K, Schonfeld K, Fondel S, Ring S, Karakhanova S, Wiedemeyer K, Bedke T, Johnson TS, Storn V, Schallenberg S, Enk AH. Depletion of CD4+CD25+ human regulatory T cells in vivo: kinetics of Treg depletion and alterations in immune functions in vivo and in vitro. *Int J Cancer* 2007;120:2723–33.
20. Ruter J, Barnett BG, Kryczek I, Brumlik MJ, Daniel BJ, Coukos G, Zou W, Curiel TJ. Altering regulatory T cell function in cancer immunotherapy: a novel means to boost the efficacy of cancer vaccines. *Front Biosci* 2009;14: 1761–70.
21. Elrefaei M, Burke CM, Baker CA, Jones NG, Bousheri S, Bangsberg DR, Cao H. HIV-specific TGF-beta-positive CD4+ T cells do not express regulatory surface markers and are regulated by CTLA-4. *Aids Res Hum Retroviruses* 2010;26: 329–37.
22. Han Y, Guo Q, Zhang M, Chen Z, Cao X. CD69+ CD4+ CD25- T cells, a new subset of regulatory T cells, suppress T cell proliferation through membrane-bound TGF-beta 1. *J Immunol* 2009;182:111–20.
23. Li R, Perez N, Karumuthil-Melethil S, Prabhakar BS, Holterman MJ, Vasu C. Enhanced engagement of CTLA-4 induces antigen-specific CD4+CD25+Foxp3+ and CD4+CD25- TGF-beta 1+ adaptive regulatory T cells. *J Immunol* 2007;179:5191–203.
24. Dunham R, Cervasi B, Brenchley JM, Albrecht H, Weintrob A, Sumpter B, Engram J, Gordon S, Klatt NR, Sodora DL, Douek D, Paiardini M, Silvestri G. CD127 and CD25 expression defines $CD4^+$ T cell subsets that are differentially depleted during HIV infection. *J Immunol* 2008; 180:5582–5592.
25. Bengsch B, Spangenberg HC, Kersting N, Neumann-Haefelin C, Panther E, Weizsacker F, Blum HE, Pircher H, Thimme R. Analysis of CD127 and KLRG1 expression on hepatitis C virus-specific $CD8^+$ T cells reveals the existence of different memory T-cell subsets in the peripheral blood and liver. *J Virol* 2007;81: 945–953.
26. Pot C, Jin H, Awasthi A, Liu SM, Lai CY, Madan R, Sharpe AH, Karp CL, Miaw SC, Ho IC, Kuchroo VK. Cutting edge: IL-27 induces the transcription factor c-Maf, cytokine IL-21, and

the costimulatory receptor ICOS that coordinately act together to promote differentiation of IL-10-producing Tr1 cells. *J Immunol* 2009;183:797–801.
27. Chen KJ, Lin SZ, Zhou L, Xie HY, Zhou WH, Taki-Elden A, Zheng SS. Selective recruitment of regulatory T cell through CCR6-CCL20 in hepatocellular carcinoma fosters tumor progression and predicts poor prognosis. *PLOS One* 2011;6:e24671.
28. Zhou J, Ding T, Pan W, Zhu LY, Li L, Zheng L. Increased intratumoralregulatory T cells are related to intratumoral macrophage and poor prognosis in hepatocellular carcinoma patients. *Int J Cancer* 2009;125:1640–8.
29. Bergmann C, Strauss L, Zeidler R, Lang S, Whiteside TL. Expansion and characteristics of human T regulatory type 1 cells in co-cultures simulating tumor microenvironment. *Cancer Immunol Immunother* 2007;56:1429–42.
30. Gregori S, Tomasoni D, Pacciani V, Scirpoli M, Battaglia M, Magnani CF, Hauben E, Roncarolo MG. Differentiation of type 1 T regulatory cells (Tr1) by tolerogenic DC-10 requires the IL-10-dependent ILT4/HLA-G pathway. *Blood* 2010; 116:935–44.
31. Gao Q, Wang XY, Qiu SJ, Yamato I, Sho M, Nakajima Y, Zhou J, Li BZ, Shi YH, Xiao YS, Xu Y, Fan J. Overexpression of PD-L1 significantly associates with tumor aggressiveness and postoperative recurrence in human hepatocellular carcinoma. *Clin Cancer Res* 2009; 15:971–9.
32. Cai MY, Xu YF, Qiu SJ, Ju MJ, Gao Q, Li YW, Zhang BH, Zhou J, Fan J. Human leukocyte antigen-G protein expression is an unfavorable prognostic predictor of hepatocellular carcinoma following curative resection. *Clin Cancer Res* 2009;15:4686–93.

Functional Characterization of Domains of IPS-1 Using an Inducible Oligomerization System

Shiori Takamatsu[1,2], Kazuhide Onoguchi[1], Koji Onomoto[3], Ryo Narita[1], Kiyohiro Takahasi[1,4], Fumiyoshi Ishidate[5], Takahiro K. Fujiwara[5], Mitsutoshi Yoneyama[3], Hiroki Kato[1,2], Takashi Fujita[1,2]*

1 Laboratory of Molecular Genetics, Institute for Virus Research, Kyoto University, Kyoto, Japan, **2** Laboratory of Molecular Cell Biology, Graduate School of Biostudies, Kyoto University, Kyoto, Japan, **3** Division of Molecular Immunology, Medical Mycology Research Center, Chiba University, Chuo-ku, Chiba, Japan, **4** Institute for Innovative NanoBio Drug Discovery and Development, Graduate School of Pharmaceutical Science, Kyoto University, Kyoto, Japan, **5** Center for Meso-Bio Single-Molecule Imaging (CeMI), Institute for Integrated Cell-Material Sciences (WPI-iCeMS), Kyoto University, Kyoto, Japan

Abstract

The innate immune system recognizes viral nucleic acids and stimulates cellular antiviral responses. Intracellular detection of viral RNA is mediated by the Retinoic acid inducible gene (RIG)-I Like Receptor (RLR), leading to production of type I interferon (IFN) and pro-inflammatory cytokines. Once cells are infected with a virus, RIG-I and MDA5 bind to viral RNA and undergo conformational change to transmit a signal through direct interaction with downstream CARD-containing adaptor protein, IFN-β promoter stimulator-1 (IPS-1, also referred as MAVS/VISA/Cardif). IPS-1 is composed of N-terminal Caspase Activation and Recruitment Domain (CARD), proline-rich domain, intermediate domain, and C-terminal transmembrane (TM) domain. The TM domain of IPS-1 anchors it to the mitochondrial outer membrane. It has been hypothesized that activated RLR triggers the accumulation of IPS-1, which forms oligomer as a scaffold for downstream signal proteins. However, the exact mechanisms of IPS-1-mediated signaling remain controversial. In this study, to reveal the details of IPS-1 signaling, we used an artificial oligomerization system to induce oligomerization of IPS-1 in cells. Artificial oligomerization of IPS-1 activated antiviral signaling without a viral infection. Using this system, we investigated the domain-requirement of IPS-1 for its signaling. We discovered that artificial oligomerization of IPS-1 could overcome the requirement of CARD and the TM domain. Moreover, from deletion- and point-mutant analyses, the C-terminal Tumor necrosis factor Receptor-Associated Factor (TRAF) binding motif of IPS-1 (aa. 453–460) present in the intermediate domain is critical for downstream signal transduction. Our results suggest that IPS-1 oligomerization is essential for the formation of a multiprotein signaling complex and enables downstream activation of transcription factors, Interferon Regulatory Factor 3 (IRF3) and Nuclear Factor-κB (NF-κB), leading to type I IFN and pro-inflammatory cytokine production.

Citation: Takamatsu S, Onoguchi K, Onomoto K, Narita R, Takahasi K, et al. (2013) Functional Characterization of Domains of IPS-1 Using an Inducible Oligomerization System. PLoS ONE 8(1): e53578. doi:10.1371/journal.pone.0053578

Editor: Karin E. Peterson, National Institute of Allergy and Infectious Diseases - Rocky Mountain Laboratories, United States of America

Received July 21, 2012; **Accepted** November 30, 2012; **Published** January 7, 2013

Funding: The Ministry of Education, Culture, Sports, Science and Technology in Japan (Innovative Areas "Infection competency" (No.24115004), Scientific Research "A"(23249023) (http://www.mext.go.jp/english/), the Ministry of Health, Labor and Welfare of Japan (http://www.mhlw.go.jp/english/index.html), the PRESTO Japan Science and Technology Agency (http://www.jst.go.jp/kisoken/presto/index_e.html), the Uehara Memorial Foundation (http://www.ueharazaidan.com/), the Takaeda Science Foundation (http://www.takeda-sci.or.jp/index.html), the Naito Foundation (http://www.naito-f.or.jp/), and Nippon Boehringer Ingelheim (http://www.boehringer-ingelheim.co.jp/com/Home/index.jsp). The funders had no role in study design, data collection and analysis, decision to publish, or preparation of the manuscript.

Competing Interests: The authors have the following interests: This study was partly funded by Nippon Boehringer Ingelheim. There are no patents, products in development or marketed products to declare. This does not alter the authors' adherence to all the PLOS ONE policies on sharing data and materials, as detailed online in the guide for authors.

* E-mail: tfujita@virus.kyoto-u.ac.jp

Introduction

Viruses replicating within cells produce RNA with a non-self signature, such as a double stranded (ds) and 5′-triphosphate structure, which are recognized by sensor molecules Retinoic acid Inducible Gene-I (RIG-I), Melanoma Differentiation Associated gene 5 (MDA5), and Laboratory of Genetics and Physiology 2 (LGP2), collectively known as RIG-I-Like Receptors (RLR) [1,2,3,4]. RLR elicits signals to activate a set of genes including those of type I and III interferon (IFN) to initiate innate antiviral responses [5]. Several lines of evidence support a hypothesis that once RIG-I and MDA5 recognize non-self RNA, conformational changes are induced resulting in exposure of their CARD [6]. The CARD of RIG-I and MDA5 transmits a signal to another CARD-containing adaptor, Interferon Promoter Stimulator-1 (IPS-1, also known as MAVS, VISA, and Cardif), which is anchored on the outer membrane of the mitochondrion [7,8,9,10]. Cells infected with a virus activate the RLR/IPS-1 signaling cascade and exhibit microscopic aggregation of IPS-1 [11]. Activation of IPS-1 is reconstituted in vitro and the formation of detergent-insoluble IPS-1 aggregate has been reported [12]. For intracellular aggregation of IPS-1, the involvement of mitofusin (MFN) 1, which is known to regulate mitochondrial fusion, has been reported [11], suggesting that IPS-1 aggregation is regulated through a complex mechanism of mitochondrial dynamics. There are several studies concerning how IPS-1 receives a signal from RLR and how it relays it downstream; however, some of the reports are not consistent with each other [10,13,14,15]. IPS-1 contains three potential TRAF binding motifs (TBMs) [10]. To avoid confusion, we refer to them as TBM1 (aa. 143–147, human),

TBM2 (aa. 154–159, human), and TBM3 (aa. 453–460, human). TBM1 and 2 are close to each other (5 amino acids apart) and reside within the proline-rich domain. TBM1 physically interacts with TRAF3 [16] and a single amino acid substitution (T147I) abolishes binding. Early reports demonstrated that an artificial molecule essentially consisting of CARD and TM, therefore devoid of TBMs (termed mini MAVS), is sufficient for signaling [9,10,13]. In particular, TM can be replaced with that of other mitochondrial proteins, suggesting the importance of its mitochondrial localization. Other reports have demonstrated that artificial oligomerization of CARD of IPS-1 in the cytosol is sufficient to activate the signal independent of the mitochondrion [14].

In the current study, we aimed to delineate the inconsistencies on the reported function of IPS-1 domains with a focus on the oligomerization of IPS-1 and analyzed the necessary part of IPS-1 for signaling.

Results

Forced IPS-1 Oligomerization Activates Antiviral Innate Immunity

Previously, we found that a virus-infection resulted in the redistribution of IPS-1 to form speckle-like aggregates in cells [11]. Here, we attempted to demonstrate whether oligomerization of IPS-1 was sufficient to induce antiviral signaling. To address this question, we modified an artificial homodimerization system (ARGENT Kit, ARIAD) [17]. We used 3 tandem repeats of mutant FK 506 Binding Protein 12 (FK_{F36V}), which can be cross-linked by a cell-permeable chemical AP20187 (Figure 1A). FK_{F36V} harbors an F36V mutation, which impairs binding affinity to immunosuppressive agent, FK506. AP20187 was designed specifically for binding with FK_{F36V}, so that it does not influence endogenous FK binding proteins. Thus, this system specifically crosslinks a target protein without the unwanted side effects. We made constructs to artificially oligomerize CARD of RIG-I in cells (FK-RIG CARD) [18] and IPS-1 (FK-IPS) (Figure 1A). HeLa cells stably expressing $3xFK_{F36V}$ (FK) and its fusion proteins were treated with AP20187 and IFN-β mRNA levels were quantified. AP20187 induced oligomerization of fusion proteins (Native PAGE, data not shown). Oligomerization of FK_{F36V} did not induce IFN-β mRNA; however, FK-RIG CARD exhibited a rapid induction of IFN-β mRNA (Figure 1B, [18]). Two independent HeLa clones expressing FK-IPS activated the IFN-β gene upon AP20187 treatment, both of which expressed the fusion protein localized to mitochondria (data not shown). Furthermore, AP20187 treatment induced speckle-like distribution of FK-IPS in cells (data not shown). It is important to note that unlike transient overexpression of IPS-1 in cell lines, which constitutively activates the IFN-β gene; stable cells did not exhibit constitutive IFN-β expression (Figure 1B). To confirm that this induction was accompanied by activation of IRF-3, its dimer formation was examined by native PAGE (Figure 1C). Consistent with IFN-β mRNA levels, cells expressing FK-RIG and FK-IPS, but not FK exhibited rapid IRF-3 dimer formation after exposure to AP20187.

To further confirm the impact of antiviral signaling by this artificial system, we examined expression profiles of interferon stimulated genes by a DNA microarray of 237 immune-related genes. 109 genes were transiently induced by IPS-1 oligomer (data not shown). Representatives 11 genes, which are known to be induced after a viral infection, are displayed in Figure 1D. Results show that a simple oligomerization of FK-RIG CARD or FK-IPS mimics the signaling induced by a viral infection (Figure 1D). In contrast, only CARD of IPS-1 failed to induce any interferon or cytokine gene expression in response to oligomerization (Figure S1). From this, it would appear that the up-regulations of these genes are not due to non-specific response induced by oligomerized CARD-containing protein.

CARD of IPS-1 is Dispensable for Oligomerization-induced Signaling

It has been hypothesized that upon activation of RIG-I, its CARD is exposed by conformational changes and relays signaling to IPS-1 through CARD-CARD interactions [8,9,10,19]. CARD of IPS-1 is essential for signaling when IPS-1 is transiently overexpressed [7,8]. We examined if CARD of IPS-1 was essential in FK-IPS-mediated signaling. We constructed FK-IPS mutants: FK-IPSΔCARD, CARD deletion; FK-IPSCARD, FK fused to CARD; FK-IPSTM, FK fused to TM, and FK-IPSΔCARDΔTM, FK-IPS without CARD and TM, as summarized in Figure 2A. Stable cells expressing FK-IPSΔCARD showed little basal activation of IRF-3; upon treatment with AP20187, strong activation of IRF-3 was observed similar to that by FK-IPS (Figure 2B). However, FK-IPS CARD did not activate IRF-3 even after oligomerization (Figure 2B). Similarly, FK-IPSΔCARD, but not FK-IPSCARD did not induce IFN-β mRNA upon oligomerization (Figure 2C). Oligomerization of FK on the mitochondrion (FK-IPSTM) is not sufficient to activate IFN-β and Interleukin(IL)-6 genes (Figure 2D, 2E). Interestingly, FK-IPSΔCARDΔTM, which is localized in the cytoplasm (Figure S2) due to TM deletions, activated IFN-β and IL-6 genes and formed speckle-like aggregates upon oligomerization (Figure 2D, 2E, and Figure S2). These results suggest that cytoplasmic oligomerization of an IPS-1 fragment (aa. 90–507), which includes TBM1–3, is sufficient for signaling and mitochondrial localization is dispensable if forcibly oligomerized.

Domain Delimitation of IPS-1 for IRF3 and NF-κB Activation

To delimit the region of IPS-1 necessary to trigger signaling upon oligomerization, we made a series of deletion mutants as shown in Figure 3A. Stable clones of HeLa cells expressing these mutants were mock treated or treated with AP20187 and nuclear translocation of IRF-3 and NF-κB was determined by immunostaining (Figure 3B). Deletion of the proline-rich region (180–540) showed little effect; however, further deletion of residues 400 to 464 abolished activation of both IRF-3 and NF-κB, indicating that these residues are essential to signal. Quantitative analysis of IFN-β and IL-6 gene expression revealed a significant attenuation of signaling by the deletion of aa. 1–179 (Figure 3C, 3D), suggesting the involvement of TBM1 and 2. This requirement of TBM1–2 is more prominent for IL-6 gene expression. Importantly, further deletion of aa. 400 to 464 (FK_{F36V}-IPS 465–540), including TBM3, resulted in the complete loss of signaling activity.

We also wondered whether MFN1 contributes to IPS-1 oligomerization because we previously reported that mitochondrial protein MFN1 promotes mitochondrial fusion and increases signaling of IPS-1 [11]. We carried out a reporter assay with this oligomerization system in MFN1−/− MEFs. MFN1−/− MEFs showed comparable level of IFN-promoter activity to WT MEF cells (Figure S3), suggesting that MFN1 is dispensable for signaling induced by forced oligomerization of IPS-1.

Essential Role of TBM3 in Signaling

To further characterize functional residues within aa. 400–540, we substituted a single amino acid within TBM3 (PEENEY to

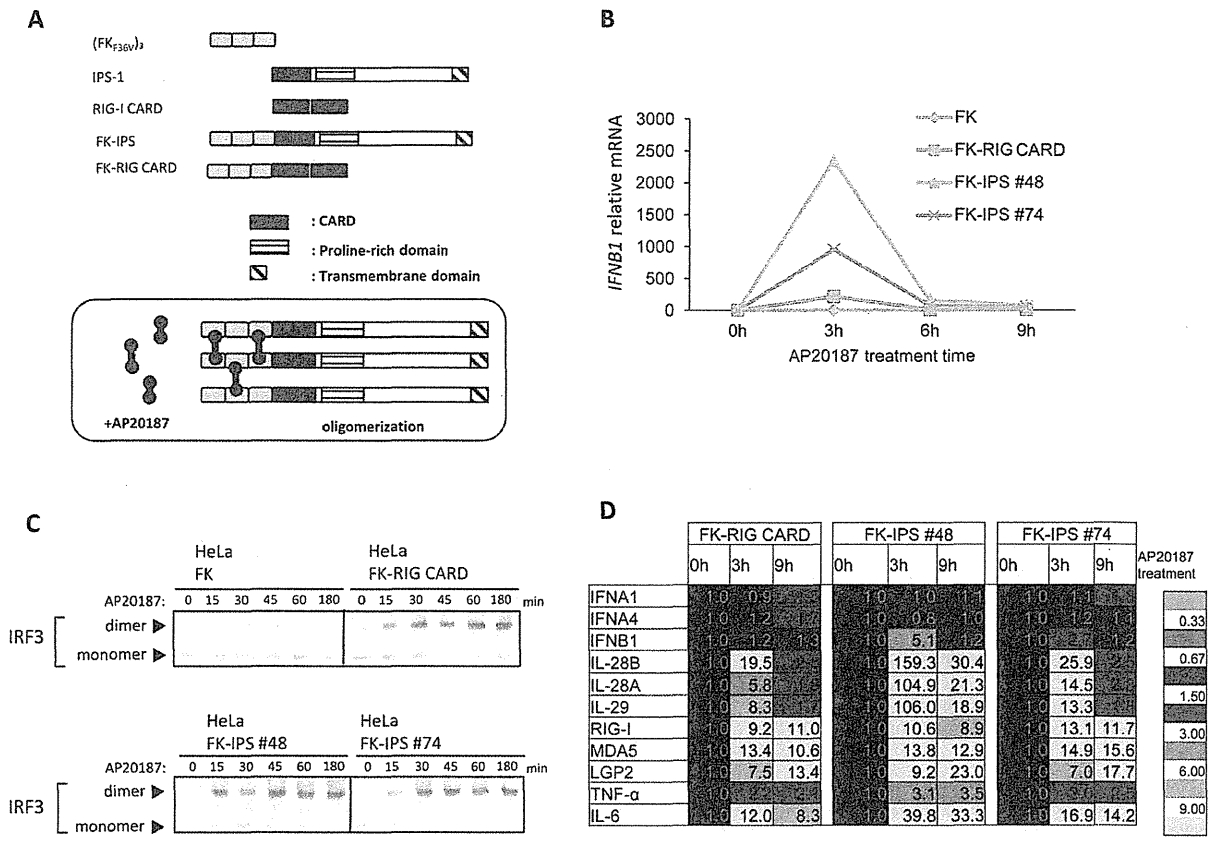

Figure 1. Forced IPS-1 oligomerization induced antiviral innate immune signaling. A. Schematic representation of FKBP fusion proteins and their oligomerization by a cross-linker, AP20187. B. HeLa cells stably expressing indicated FKBP fusion proteins were treated with AP20187 (10 nM) for the indicated time. Cells were harvested and analyzed for IFN-β mRNA levels by qPCR. C. HeLa cells stably expressing indicated FKBP fusion proteins were stimulated with AP20187 for 3 h and IRF-3 dimer formation was analyzed (Materials and Methods). Positions of the IRF-3 monomer and dimer are shown by arrowheads. D. Microarray analysis of mRNAs induced by oligomerized RIG-I CARD or IPS-1. Cells were stimulated with AP20187 for the indicated time. Total RNA extracted from these cells was subjected to analysis using a DNA microarray (Genopal, Mitsubishi Rayon) of interferon-stimulated genes and interferon genes. Relative mRNA levels using a control expression as 1.0 are shown. Representative data of at least two independent experiments are shown.
doi:10.1371/journal.pone.0053578.g001

PEDNEY: E457D) [10] to explore its significance (Figure 4A). E457D substitution abolished gene activation of IFN-β and IL-6 with full-length or 400–540 FK_{F36V} fusion constructs in stable HeLa cells (Figure 4B, 4C). We confirmed that IRF and NF-κB were activated by oligomerization of IPS-1 400–540 in a TBM3-dependent manner (Figure 4D, 4E). We further mutagenized TBM3 to resemble TBM of Toll/IL-1 receptor domain-containing adaptor inducing IFN-β (TRIF) (PEEMSW) or IL-1 receptor-associated kinase (IRAK)-M (PVEDDE). As a negative control, the motif was replaced to that of Myeloid Differentiation factor 88 (MyD88) (PSILRF), which does not bind directly to the TRAF molecule [20]. Interestingly, substitution of TBM3 with TBM of TRIF or IRAK-M restored the induction of IRF3 and NF-κB, albeit with lower efficiency (Figure 4F, 4G). As expected, the control motif of MyD88 failed to exhibit signaling. Furthermore, we constructed FK-IPS 400–508, which retains TBM3 but lacks the TM. This short fragment of IPS-1 also activated IRF-responsive promoter upon oligomerization(Figure S4). This result further supports the hypothesis that oligomerization of TBM3 is essential in IPS-1 mediated signaling.

Viral Infection Induces Molecular Oligomer of IPS-1

The above results show that forced oligomerization of IPS-1 results in the activation of a signaling cascade. We investigated if a viral infection induced oligomerization of IPS-1 using fusion proteins of complementary fragments of a fluorescent reporter protein (monomeric Kusabira-Green, mKG) [21]. Two split inactive mKG fragments fused to IPS-1, respectively, were expressed in cells. Fluorescence is expected to be detectable when these IPS-1 fusions containing complementary mKG fragment came into close vicinity (Figure 5A). 293T cells, which stably expressed mKG-fusion IPS-1, were infected with Newcastle disease virus (NDV) for 9h and then subjected to Fluorescence-Activated Cell Sorting (FACS) analysis for the detection of fluorescence. We observed enhanced fluorescence in NDV-infected cells (Figure 5B), suggesting that viral infections induce oligomer formation of IPS-1.

Discussion

Signaling initiated by cytoplasmic viral RNA sensors involves a unique adaptor, IPS-1, which is specifically expressed on the outer

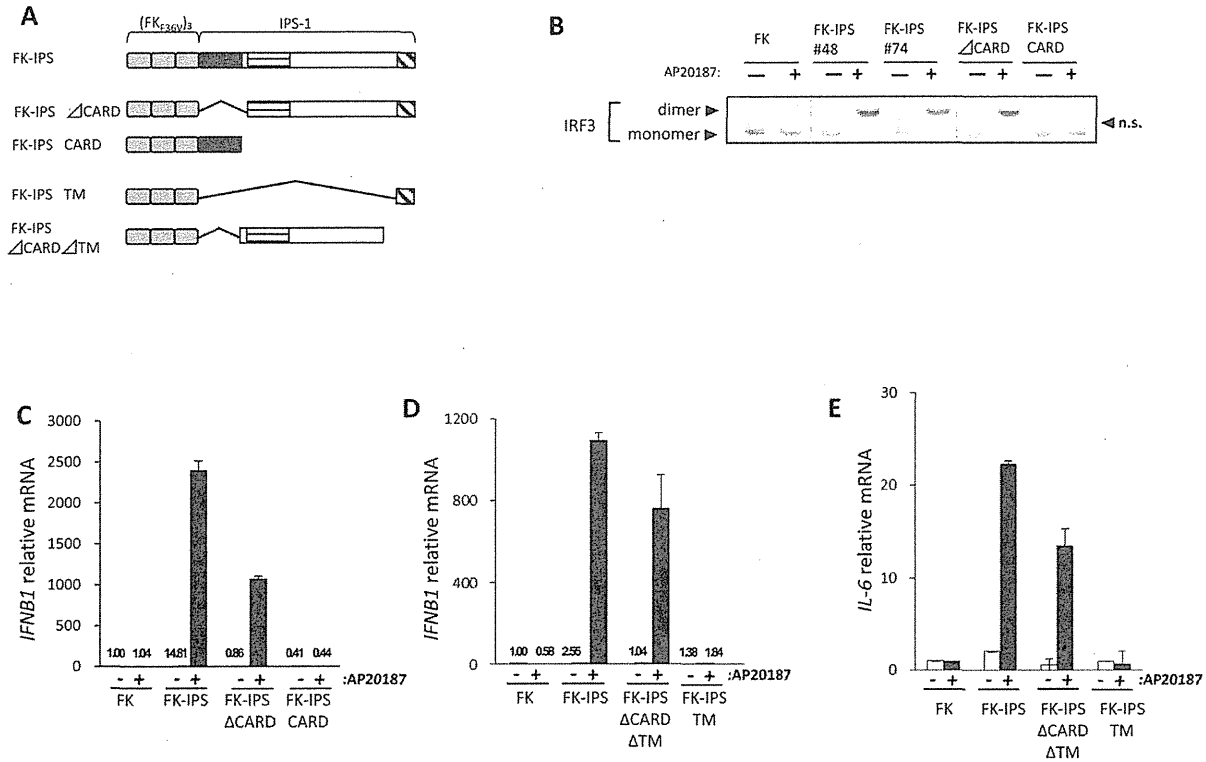

Figure 2. CARD of IPS-1 is dispensable for oligomerization-induced signaling. A. Schematic representation of FK-IPS deletion mutants. B. HeLa cells stably expressing indicated FK-IPS fusion were mock treated or treated with AP20187 for 3 h. Cell lysates were analyzed for IRF-3 dimer formation as in Figure 1C. n.s.: non-specific band. C–E. Indicated HeLa cells stably expressing FK-IPS constructs were mock treated or treated with AP20187 for 3 h. Cellular RNA were extracted and analyzed for IFN-β (C, D) or Il-6 (E) mRNA by qPCR. Representative data of at least two independent experiments are shown. Error bars: standard error of triplicated samples.
doi:10.1371/journal.pone.0053578.g002

membrane of the mitochondrion. IPS-1 is a problematic protein, since transient overexpression results in constitutive signaling, whereas endogenous IPS-1 is tightly regulated by post-translational mechanisms [22,23]. Here, we established a system to analyze the regulation of IPS-1 by its oligomerization. We obtained stable cell lines expressing FK-IPS fusion, which could be activated by a crosslinker. Upon oligomerization, IPS-1 rapidly elicited signaling leading to the activation of target genes including that of IFN-β, suggesting that IPS-1 aggregation is essential and precedes possible covalent modifications such as phosphorylation and ubiquitination [24,25].

Our deletion analysis of FK-IPS-1 revealed that the TRAF binding motif is essential while CARD is dispensable for signaling. The initial report by Chen's group reported that CARD tethered to mitochondria-targeted TM (termed mini MAVS) is sufficient to transduce signaling by its transient overexpression [9,13]. They expressed mini-MAVS in cells expressing endogenous IPS-1. However, when mini-MAVS was expressed in IPS-1−/− cells, no signal was transduced (Figure S5, [26]). And recently Chen's group also reported that depletion of endogenous IPS-1 by RNAi abrogated interferon induction by mini-MAVS [12]. This can be interpreted as transient overexpression of CARD in the vicinity of mitochondria resulting in the aggregation of endogenous IPS-1. In contrast, FK-IPS 400–450, which lacks CARD, is regulated by oligomerization in IPS-1−/− MEFs (Figure 4D, 4E). Another group showed that cytoplasmic oligomerization of CARD is sufficient to activate signaling using FK fusion [14]. This result is clearly inconsistent with ours (Figure 2B, 2C). They used wild type FKBP12 and dimerizer chemical AP1510, which retains its binding affinity to endogenous FKBP proteins. One of the FKBPs, FKBP38 (also termed FKBP8) is known to associate with the mitochondrial outer membrane [27]. Therefore, this primordial oligomerization system may oligomerize the target proteins (this case CARD) in association with mitochondria. We used an improved FKBP system (ARGENT Kit, ARIAD), which avoids this potential problem. On the other hand, FK-IPS ΔCARDΔTM, which contains TBMs, can activate signaling upon oligomerization (Figure 2). This result highlights the fact that cytoplasmic oligomerization of TBMs is sufficient for signaling.

There are three potential TBMs within IPS-1 [10]. Our result showing that FK-IPS 400–540 exhibited signaling in an oligomerization-dependent manner (Figures 3 and 4) suggest that oligomerization of TBM 3 alone is sufficient for signaling. TBM3, initially identified as TRAF6 binding site [10], can also recruit TRAF3 [28]. This is consistent with studies using TRAF3 and TRAF6 knockout cells [29,30]. TBM1, 2, and 3 likely contribute to the signaling mediated by IPS-1, presumably in a cooperative fashion and result in differential activation of target genes. For example, TBM1 and 2 are dispensable for the IFN-β gene, but IL-6 gene requires all TBM1, 2, and 3 for full activation (Figure 3C, 3D). A recent report has shown that CARD containing protein CARD9 is preferentially required for

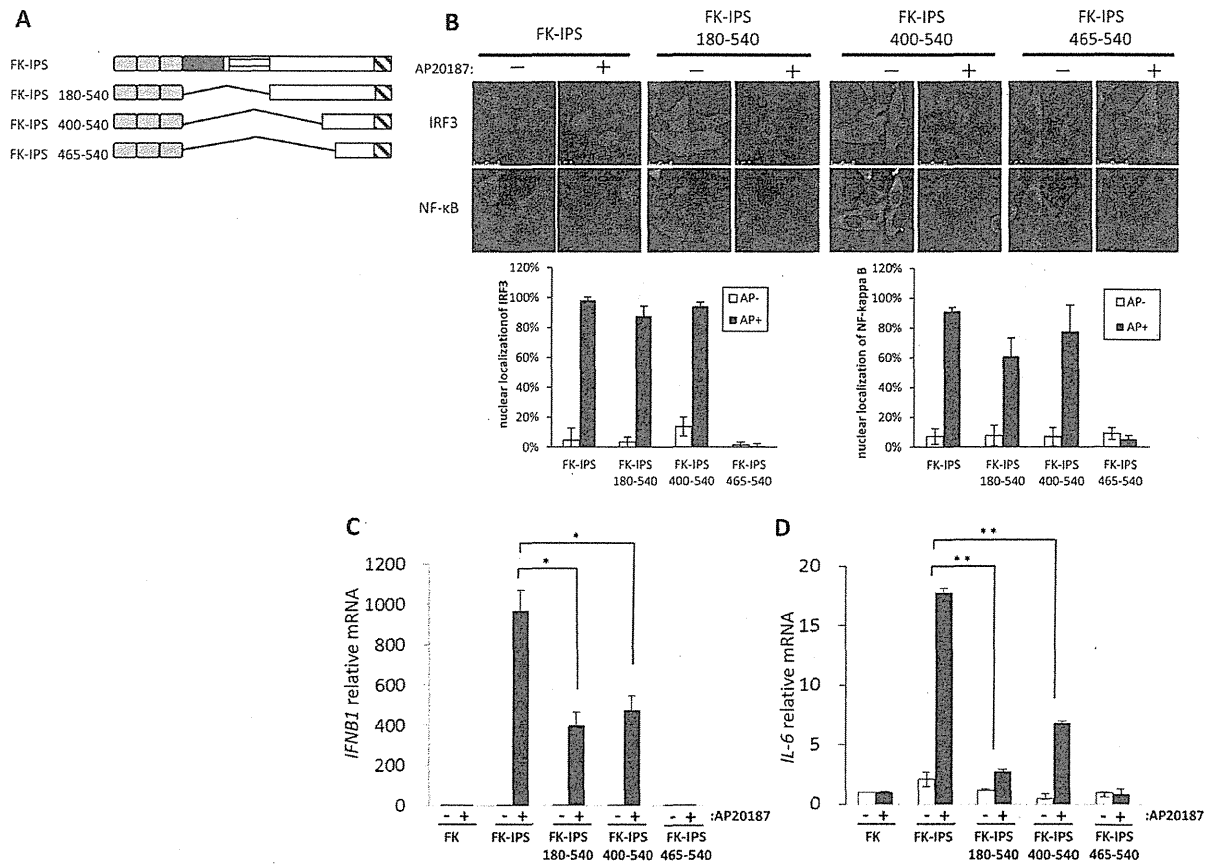

Figure 3. Delimitation of critical domain in IPS-1 for IRF3 and NF-κB activation. A. Schematic representation of FK-IPS deletion mutants. B. HeLa cells stably expressing indicated FK-IPS deletion mutants were mock treated or treated with AP20187 for 3 h. Cell were fixed and stained for IRF-3 and NF-κB p65, respectively. Fluorescent microscopic images of IRF3 and NF-κB staining are shown (top). The percentage of cells with nuclear IRF-3 or NF-κB was determined by counting 100 cells (bottom). C, D. Cellular RNA was extracted and analyzed for IFN-β (C) or IL-6 (D) mRNA by qPCR. Representative data of at least two independent experiments are shown. Error bars: standard error of triplicated samples. Statistical analyses were conducted with an unpaired t test, with values of $p<0.05$ considered statistically significant. *$p<0.05$, **$p<0.005$.
doi:10.1371/journal.pone.0053578.g003

proinflammatory cytokine induction downstream of RIG-I signaling [31]. To explore the involvement of CARD9 in IPS-1 mediated signaling, we knocked down CARD9 in a stable HeLa clone expressing FK-IPS and examined its effect on the activation of IFN-β and IL-6 genes (Figure S7). Although IFN-β gene induction by oligomerization was little affected by reducing CARD9, IL-6 gene activation was significantly attenuated. Considering the result that IL-6 gene activation is more dependent on TBM1/2 (Figure 3C, 3D), it is tempting to speculate that TBM1/2 preferentially promote NF-κB activation, whereas TBM3 has a primary role of IRF-3/7 activation.Our results support a model that CARD of IPS-1 receives signaling from RLR via CARD-CARD interaction to initiate oligomerization through mitochondrial dynamism; however, CARD of IPS-1 alone is not sufficient to trigger downstream signaling. On the other hand, TBMs are essential for further signaling by the recruitment of TRAF3 and 6, which is initiated by molecular oligomerization. Consistent with this model, we observed that artificial oligomerization of IPS-1 induced recruitment of TRAF6 into the NP-40-insoluble fraction (Figure S6). Thus, IPS-1 receives and transmits signaling through the functions of CARD and the TRAF motif, respectively.

Materials and Methods

Plasmid Constructs

p-55C1BLuc, p-55A2Luc, p-125Luc, pRLtk, pEF-Bos-FLAG-RIG-I CARD and pEF-Bos-FLAG-IPS-1 plasmids have been described [11,32]. Expression plasmids of FKBP36v (oligomerization peptide), pC4M-Fv2E, and pC4Fv1E were obtained from ARIAD (ARGENT Regulated Homodimerization kit). We reconstructed the vector, pC4Fv3E, which contains 3 tandem repeats of FKBP36v [18]. To construct IPS-1 fused three tandem FKBP, we amplified the IPS-1 sequence by PCR and inserted it into the SpeI site of pC4Fv3E. Site-directed FK-fused IPS-1 mutants (FK-IPS E457D, FK-IPS 400–540 E457D) were constructed using a KOD-Plus mutagenesis kit (TOYOBO, Japan). Nucleotide sequences for these constructs were confirmed with the BigDye DNA sequencing kit (Applied Biosystems). Expression vectors encording Flag-MAVS and Flag-mini-MAVS were obtained from Dr. Zhijian J. Chen.

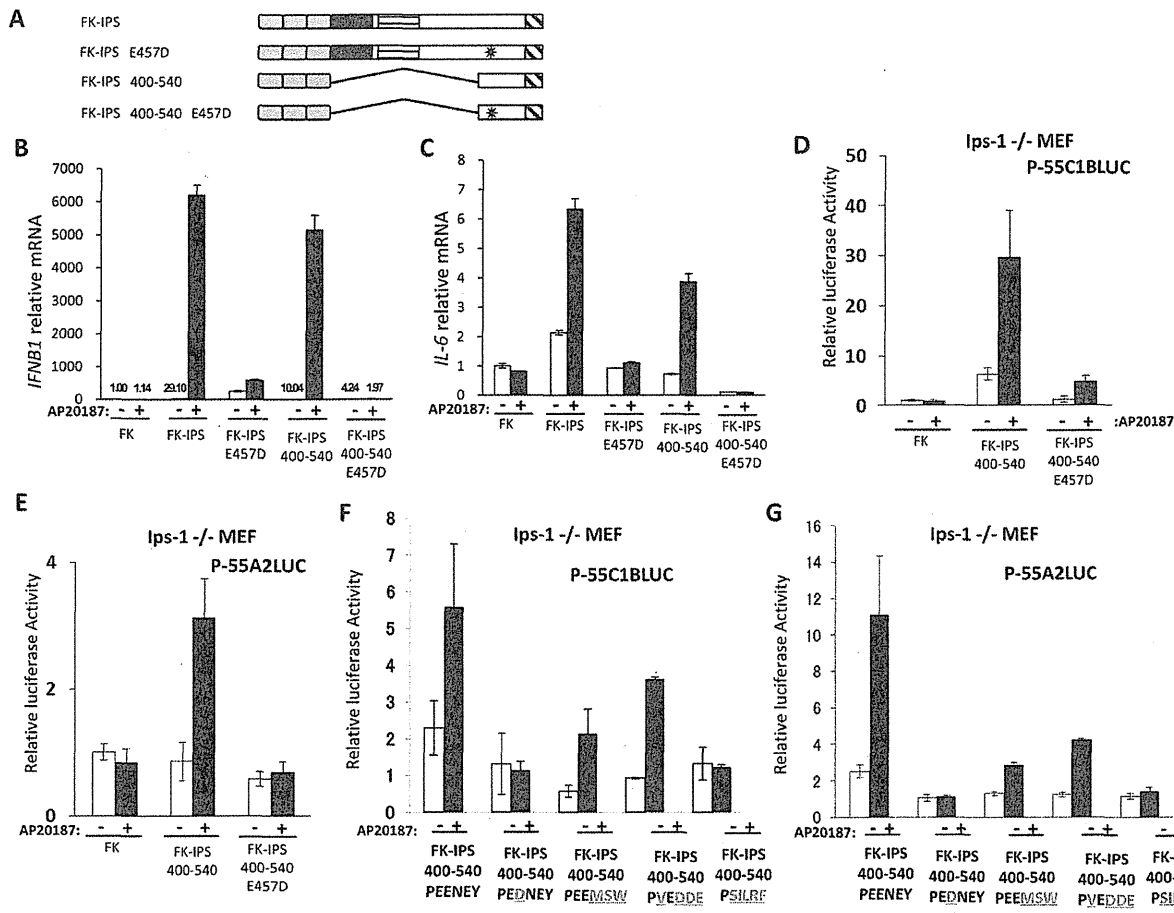

Figure 4. Essential role of TBM3 in signaling. A. Schematic representation of FK-IPS fusion proteins. Asterisks represent the point mutation. B, C. HeLa cells stably expressing indicated FK-IPS mutants were mock treated or treated with AP20187 for 3 h. Cellular RNA were extracted and analyzed for IFN-β (B) or IL-6 (C) mRNA by qPCR. D–G. IPS-1−/− MEFs were transiently transfected with the luciferase reporter plasmid, p-55C1BLuc (for IRF, D, F) or p-55A2Luc (for NF-κB, E, G), together with indicated FK-IPS-1 fusion constructs. For TBM3 mutants, substituted amino acids are shown as red letters (F, G). Cells were treated with or without AP20187 for 6 h. Relative luciferase activities were determined as described in the Materials and Methods. A representative result of at least two independent experiments is shown. Error bars: standard error of triplicated samples.
doi:10.1371/journal.pone.0053578.g004

Cell, DNA Transfection, and Preparation of Cell Extracts

HeLa, 293T cells [32,33] and Mouse embryonic fibroblasts (MEFs) [5,34] were maintained in Dulbecco's Modified Eagle's Medium with 10% fetal bovine serum and penicillin-streptomycin. MEFs deficient for IPS-1 were obtained from Dr. S. Akira (Osaka University). MEFs deficient in MFN1 were obtained from Dr. David Chan (Caltech). HeLa, 293T cells, and MEFs were transfected with FuGENE 6 (Roche Applied Science). Stable transformants of HeLa cells were established by transfection of linearized plasmids, encoding the FKBP construct and Puromycin resistance gene, respectively, and cells were selected by Puromycin (5 μg/ml). For preparation of cell extracts, cells were lysed with lysis buffer (50 mM Tris-HCl pH 7.5, 150 mM NaCl, 1 mM EDTA, 1% Nonidet P-40, 0.1 mg/ml leupeptin, 1 mM phenylmethylsulfonyl fluoride, and 1 mM sodium orthovanadate) and were centrifuged at 20400×g for 10 min. The supernatant was used for immunoblotting.

Viral Unfection

Cells were treated with culture medium or infected with NDV at a MOI of 1 in serum-free and antibiotic-free medium. After adsorption for 1 h at 37°C, the medium was changed and infection was continued for 9 h in the precence of serum-containing medium.

Reporter Assay

MEFs were transfected with firefly luciferase reporter (either p-125 Luc, p-55C1BLuc or p-55A2Luc [32]) pRLtk (renilla luciferase internal control) and effector expression plasmids. Cells were split into three aliquots and were stimulated with chemical dimerizer AP20187 (AP, 10 ng/ml in ethanol) or ethanol. The luciferase assay was performed with a Dual-Luciferase reporter assay system (Promega). Luciferase activity was normalized using *Renilla* luciferase activity (pRLtk).

Quantitative Real Time PCR and Microarray Analysis

Total RNA was prepared with TRIZOL reagent (Invitrogen) and treated with DNase I (Roche Diagnostics). A High-Capacity